Letters in Applied NanoBioScience
Open-Access Journal (ISSN: 2284-6808)

Review
Volume 12, Issue 3, 2023, 88
https://doi.org/10.33263/LIANBS123.088

Thermostability of Selected Biological Materials

Bartosz Leśniewski [1,2,*], Martyna Kotula [1,2], Anita Kubiak [1,2], Martyna Pajewska - Szmyt [2,*]

[1] Faculty of Chemistry, Adam Mickiewicz University, Uniwersytetu Poznańskiego 8, 61-614 Poznań, Poland; barles5@amu.edu.pl (B.L.); markot6@amu.edu.pl (M.K.); anikub@amu.edu.pl (A.K.);
[2] Center for Advanced Technologies, Adam Mickiewicz University, Uniwersytetu Poznańskiego 10, 61-614 Poznań, Poland; mpszmyt@amu.edu.pl (M.P-S.);
* Correspondence: barles5@amu.edu.pl (B.L.); mpszmyt@amu.edu.pl (M.P-S.);
Paper dedicated to Professor Hermann Ehrlich on the Occasion of His 65th Birthday.

Scopus Author ID: 57205603979

Received: 16.02.2022; Accepted: 28.03.2022; Published: 22.05.2022

Abstract: Thermostability is a crucial property of biological materials, especially in the case of their potential application in materials science, including such novel directions as Extreme Biomimetics. This approach includes research at high temperatures without destroying the 3D structure of selected biological materials that allow the development of novel nanostructured composites. Consequently, this article presents an overview of the characterization of such biomaterials as chitin, chitosan, spongin, collagen, keratin, silk, byssus, and conchiolin in the contest of their structure and thermostability with respect to future potential applications. The review also highlights the instrumental techniques used for thermal analysis of materials – thermogravimetric methods. The review covered the latest achievements in the issue of thermostability research of natural, renewable materials, and the information presented in this paper may be valuable in future practical studies.

Keywords: thermostability; biological materials; biomaterials; chitin; chitosan; keratin; spongin; collagen; cellulose; silk.

1. Introduction

A biomaterial is every material used to produce devices that substitute a part or function of the body in a secure, reliable, economical, and physiologically acceptable manner [1,2]. The definition of biomaterial is suggested by the European Society for Biomaterials Consensus Conference II: “A biomaterial is a material intended to interface with biological systems to evaluate, treat, augment or replace any tissue, organ or function of the body” [1,3]. The Clemson University Advisory Board for Biomaterials has identified a biomaterial as “a systemically and pharmacologically inert substance designed for implantation within or incorporation with living systems” [1,2,4]. Due to their wide application in medicine, biomaterials must be sterilizable and, consequently, thermostable [4–6]. The classification of biomaterials is shown in Figure 1.

The purpose of sterilization is to get rid of all kinds of microorganisms that could cause infections. Several basic sterilization methods include gamma irradiation, steam, ethanol, or gas (ethylene oxide) sterilization. The method used depends on the type of material, as some materials may release toxic products during sterilization, e.g., some polymers such as polyacetal release toxic formaldehyde during gamma irradiation. Thermal analysis of materials also provides information on the sterilization method of such material, which can be used so as not to damage its structure [1–4,7–9].

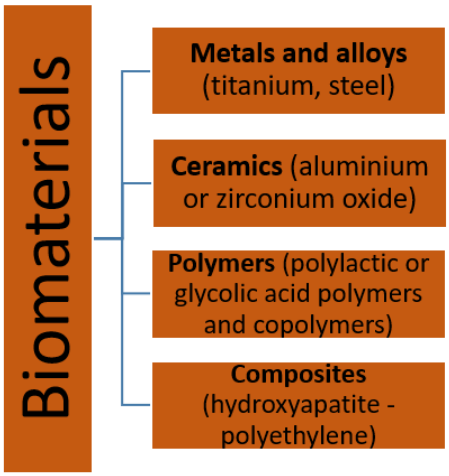

Figure 1. Classification of biomaterials (according to [4]).

Biological materials (i.e., bones, cellulose, spongin, collagen, silk, keratin, chitin, conchiolin, dentin) are produced only by biological systems [1]. There are several differences between biological materials and their artificial substitutes - biomaterials. Apart from the difference in the viability of biological materials, they are mostly immersed in body fluids. In addition, biological materials are considered nanostructured composites [1,2,4,10].

The rapid development of modern biomaterialogy is also due to sustainability, thanks to the use of naturally occurring and renewable biopolymers [1,6,11–16]. The renewable, structural biological materials discussed in this review, from the view of their thermostability, allow the use of naturally occurring biological structures to construct new composites to improve their physicochemical and material properties while maintaining their essential characteristics [17]. As a result, innovative materials are created with a number of potential applications, including bioinspired materials science [18] and extreme biomimetics [5,19,20]. According to the modern view [21], "Extreme biomimetics in materials science can be defined as the search for natural biomaterial sources outside the human comfort zone (temperature, toxicity, pH, salinity, pressure, etc.) for engineering inspiration to create inorganic-organic hybrid composites resembling their unique properties". Thermostability of biological materials remains one of the key features for their future applications within the approach, which belong to extreme biomimetics and hydrothermal synthesis of hybrid composites.

2. Thermogravimetric Analysis

There are three most important techniques for thermal analysis of materials: Differential Scanning Calorimetry (DSC), Differential Thermal Analysis (DTA), and Thermogravimetry Analysis (TGA). The DSC measures the energy changes that occur when the sample is heated or cooled and the temperature at which these changes occur. This method is widely used to measure thermal stability, e.g., of polymers, drugs, glass, proteins, and other materials. DTA is a technique similar to DSC in which a test sample and a neutral reference sample are analyzed in the same thermal cycles. Then a graph is created containing the temperature difference as a function of time or temperature. This technique is most commonly used in the pharmaceutical, food, and environmental research industries [5,22–24]. TGA is the most commonly used method to analyze the thermal stability of materials. Currently, more modern methods of measuring the thermal stability of materials are also known, including Thermomechanical Analysis (TMA), Dynamic Mechanical Analysis (DMA), and Dielectric Analysis (DEA).

TMA measures the deformation of a material under a constant load as a function of temperature while the material is in a temperature-controlled program. Thanks to the DMA analysis, it is possible to determine the mechanical properties of the sample, e.g., the glass transition temperature of the material as a function of temperature and frequency simultaneously. With DEA, the capacity and conductivity of a material can be measured as a function of time (most commonly used for thermoplastics, thermosets, composites, adhesives, and coatings) [24]. By reviewing the thermal stability of several important and increasingly widely used materials, conclusions about their resistance at various temperatures and the range of possible applications can be drawn, including biomedical and industrial ones.

TGA analysis is extremely useful for examining polymeric materials, composites and fibers. It provides information on the loss of the sample mass as a function of temperature or time increase. Thanks to this, it is possible to easily determine the thermal stability of the material, i.e., the maximum temperature at which a given material can be used and oxidative stability (rate of oxygen absorption on the material) [5,24–27]. Knowledge of thermostability and degradation kinetics is useful for planning and optimizing diverse industrial processes [24,28]. The change in sample weight results from thermal decomposition and the emission of gaseous products such as water and carbon dioxide. Sublimation or oxidation processes also take place. The main advantages of TGA are short analysis time and its simplicity, a small amount of sample needed to perform the analysis, and control over the course of the analysis throughout its duration. TGA analysis is performed using a thermogravimeter whose structure is shown in Figure 2.

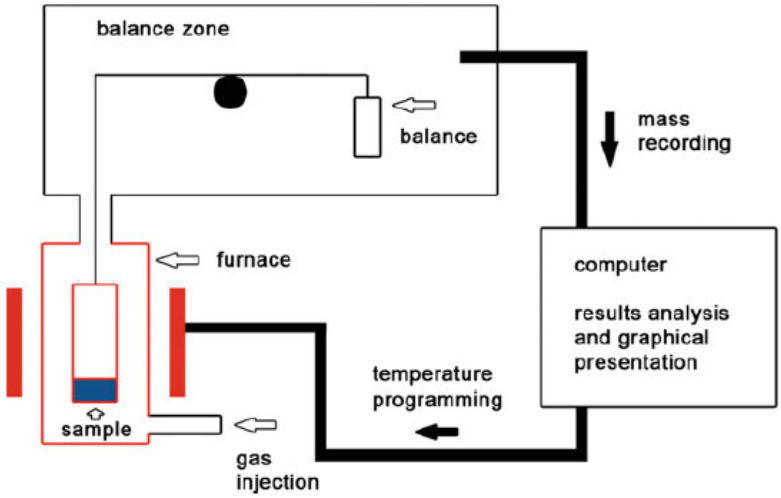

Figure 2. Schematic diagram of a thermogravimeter [5]. Reprinted by permission from [Springer Nature Customer Service Centre GmbH]: Springer Nature [Extreme biomimetics] (Editor: Hermann Ehrlich) [Chapter 7: Thermogravimetric Analysis of Sponge Chitins in Thermooxidative Conditions] by Dawid Stawski [COPYRIGHT] (2017).

The sample is placed in an oven connected to a thermobalance, and heating to the required temperature is started (measured with a thermocouple). The sample is placed in an appropriate holder made of aluminum or platinum (material that is thermostable and non-reactive under the TGA analysis conditions), which ensures that the entire sample is heated under the same conditions. The analysis may be carried out under an inert atmosphere, e.g., nitrogen or argon, or in an oxidizing atmosphere (oxygen). The rate of decomposition depends on the rate of heating (the faster the heating, the higher the decomposition temperature – 10

°C/min is often used). The sample mass is then plotted against temperature or time using appropriate software [5,23,27].

3. Thermostability of Selected Biological Materials

3.1. Cellulose.

Cellulose is a natural biopolymer that belongs to structural polysaccharides made of D-glucose molecules linked by glycosidic bonds. It is found in the cell walls of plants and some algae, fungi, and bacteria. The properties of native cellulose mainly depend on the isolation process, the number of hydrogen bonds, chain length, crystallinity, and the distribution of functional groups in the chain - all these parameters give cellulose many unique properties [29,30]. Cellulose has many practical applications: cellulose-based paper is used as electrical insulation in cables and transformers. Cellulose esters are used in partition membrane materials [31,32]. This biopolymer is also of great importance in the textile industry - cotton used to make clothes consists of about 94 % cellulose [33]. In turn, bacterial cellulose (obtained from microorganisms, e.g., Gram-negative species of the genus Gluconacetobacter, Sarcina, Azobacter Achromobacter, Aerobacter, Salmonella, Rhizobium, Pseudomonas, and Alcaligenes), due to its biocompatibility, mechanical properties (resemble human tissues) and its microstructure, is used in biomedicine, regenerative medicine, and tissue engineering. In addition, bacterial cellulose is used in wound healing, as biosensors, and in the cosmetics industry. Despite the high production costs, bacterial cellulose is produced on an industrial scale in accordance with the principles of green chemistry due to its unique properties and possible biomedical applications [34].

Cellulose nanocrystals with unique physicochemical properties are extremely popular, and they occur naturally and do not need to be synthesized [35,36]. Cellulose nanocrystals modified with sulfates and crystallized with sulfuric acid show low thermal stability. Studies are available in the literature showing an easy method of sulfate removal and final treatment of the resulting powder, e.g., acid gelling, the use of ethanol as a solvent, or drying with supercritical carbon dioxide. As a result, the dispersibility of the nanocrystalline cellulose powder is restored, and thermal stability is improved. Such a powder is widely used in the production of nanocomposite materials, optoelectronics, tissue scaffolds, biosensors, energy storage devices, and catalysts [37].

It has been shown that cellulose nanocrystals hydrolyzed with phosphoric acid have higher thermal stability than hydrolyzed with sulfuric acid. The density of the surface charge in the acid form determines the thermostability of the western processes of de-esterification and degradation. Sodium nanocrystals of cellulose do not influence thermostability, which is proved in the literature [38]. Microfibrillar cellulose fibers are the most thermostable, despite the presence of many amorphous regions. On the other hand, acidic cellulose nanocrystals containing sulfates on the surface undergo degradation already at a temperature below 200 °C, while cellulose nanocrystals neutralized with sodium ions have higher thermal stability, up to about 300 °C [30]. The thermal stability of cellulose nanocrystals is very close to that of cellulose, which is well described in the literature [35,36]. Cellulose has a fairly high thermostability due to its crystallinity and a closed structure that hinders the heat flow caused by the high energy of hydrogen bonds. Higher extractive content results in lower cellulose crystallinity and smaller crystallite size. This leads to faster thermal degradation and lowers the thermal stability of lignocellulosic fibers, as confirmed in the available literature. Due to the

use of methods that allow the identification of the structure and size of crystallites in advance (FT-IR, XRD), it is possible to increase the thermal stability of the obtained composites [29]. Natural fiber reinforced nanocellulose is used in the production of thermoplastic composites. The physicochemical and thermal properties of nanocellulose are affected by crystallinity, which depends mainly on the source and method of cellulose treatment. Moreover, the degree of polymerization and the drying method affect the thermal degradation of cellulose samples [38,39]. A commonly used reaction is the oxidation of cellulose because the products of this process are of great importance in pharmacy, biomedicine, food and cosmetic industries, and polymer composites. The carboxyl and aldehyde groups present in cellulose greatly influence its thermal stability. According to the literature, 2,3-dialdehyde cellulose is the most thermostable. Reducing carboxyl groups located at the end of the polymer chain have a strong destabilizing effect on the thermal stability (the carboxyl group in the C6 position of cellulose reduces the thermal stability of the oxidized cellulose products). The difference in the thermal stability of these products is great since the cellulose-containing the C6 carboxyl groups begin to decompose at 172 °C, while the 2,3-dialdehyde cellulose only at 308 °C. To obtain the cellulosic material with the best thermostability, no carboxyl groups must be present at the C6 position in the polymer chain, and their presence as reducing end groups must be obscured [40].

Thermogravimetric tests of cellulose are of great practical importance because, thanks to them, it is possible to determine the service life of insulation and membrane systems to produce energy from biomass and chemical agents that reduce the flammability of cellulose fibers [25,32]. Thermal degradation of cellulose and its compounds in nitrogen consists of a series of reactions, such as dehydration and pyrolysis of the cellulose skeleton. Below 300 °C, decomposition of glycosyl units occurs due to the loss of water, carbon dioxide, and carbon monoxide. Between 300 and 600 °C cellulose is depolymerized [25,31,33,35,41,42]. At 400 °C, about 90 % of the cellulose is degraded, and the decomposition of the entire sample takes place at about 700 °C. Nitro and sulfate groups favor faster degradation of cellulose, while acetate groups significantly improve the thermal stability of cellulose. The thermal decomposition of cellulose in the air atmosphere takes place much faster because the oxygen present in the air acts as a catalyst accelerating the decomposition of cellulose. Therefore, an increase in the oxygen content reduces the thermal stability of cellulose [32,43,44]. The comparison of temperatures for individual stages of thermal decomposition of cellulose in nitrogen and air atmosphere is presented in Table 1.

Table 1. The comparison of temperatures for individual stages of thermal decomposition of cellulose in nitrogen and air atmosphere (based on [25,32,42]).

	In nitrogen	**In air**
Dehydration	below 100 ºC	below 100 ºC
Pyrolisis of the skeleton	400 ºC	360 ºC
Oxygen catalysis	———	475 ºC
Complete degradation	700 ºC	670 ºC

Comparing natural and regenerated cellulose fabrics, it can be noticed that regenerated fabrics, e.g., viscose, are subject to thermal degradation faster due to the lower degree of polymerization. On the other hand, natural fabrics, such as linen or cotton, are more thermostable [33]. To improve the mechanical and thermal properties of bacterial cellulose to make composites for biomedical applications, collagen has been used and described in the literature. As a result of mixing BC in the form of films or powder with a collagen solution and

subsequent freeze-drying, a product with much better thermostability is obtained, while as a result of mixing with collagen gel, composites with unique properties are obtained. These studies proved that collagen has a positive effect on microbial cellulose's thermal stability and mechanical characteristics. Bacterial cellulose is degraded in the range of 250-350 °C, while BC modified with collagen solution is the most thermostable - its degradation takes place in the range of 275-400 °C (only 25 % of the sample weight is lost at temperatures up to 400 °C) [45]. The high thermal stability of cellulose and many known methods of its improvement make this biopolymer used as insulation paper in power transformers and is a big competition for low-ecological plastics. In order to improve the thermal stability of cellulose, the cyanoethylation reaction is most often used to replace some of the hydroxyl groups with more stable ones and less prone to thermal degradation. During the degradation of cellulose modified in this way, less water is also produced, promoting degradation, and accelerating the hydrolysis reaction. Replacing polar groups with nonpolar ones deteriorates the mechanical properties. To avoid this, nitrogen-containing additives are used, e.g., urea, dicyandiamide, and polyacrylamide. The basic additives neutralize the carboxylic acids formed during the degradation, remove the formed water molecules and ensure the stabilization of the reducing end groups. The only drawback of such additives is the formation of toxic and corrosive ammonia [46].

3.2. Chitin.

Chitin is a naturally occurring structural polysaccharide composed of N-acetyl-D-glucosamine units [47]. Chitin differs from cellulose by using an acetamide group instead of a hydroxyl group at the C2 position of the glucose unit [26,48–50]. It has a highly ordered crystal structure [51], making it necessary to use methods that lower the crystallinity to synthesize its derivatives, e.g., gamma radiation and ultrasound. As a template for skeleton's rigidification and biomineralization [52,53], chitin has been found in diverse species of yeast, fungi, and diatoms [54], as well in the exoskeletons of corals [55,56], marine and fresh water sponges (Figure 3) [57–61], as well as in all arthropods [62,63]. Unfortunately, in the case of marine crustaceans, chitin is one of the main pollutants in coastal areas. β-chitin obtained from squid is more reactive and more soluble than α-chitin obtained from shrimps and crabs due to weaker intermolecular hydrogen bonds. It is much easier to deacetylate to form more useful chitosan [28,64,65].

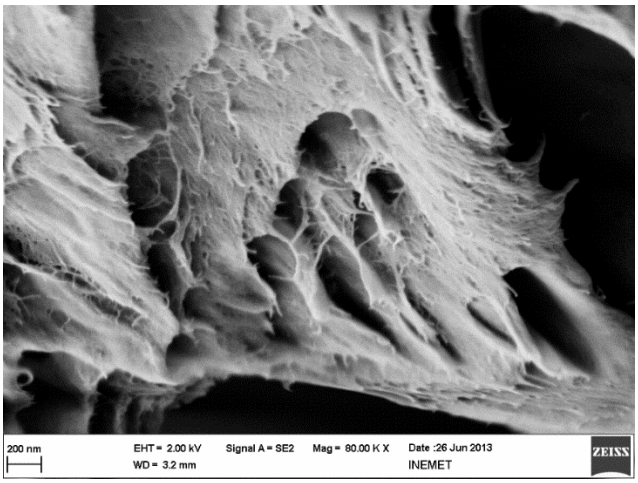

Figure 3. SEM image representing the nanostructural organization of chitin isolated from *Aplysina fistularis* demosponge.

Chitin and its derivatives are very important in materials science, materials engineering, agriculture, chemistry, biochemistry, food and feed additives, biomedicine, and environmental science [66]; therefore, the synthesis of derivatives of this polysaccharide is still on trend [26,64,65,67,68]. Currently, chitin is an alternative to plastics. Moreover, research is ongoing on naturally pre-structured chitin scaffolds obtained from sponges for their implementation in regenerative medicine or environmental science [66]. Due to the biodegradability, biocompatibility, and non-toxicity of chitin, large-scale research is carried out on chitin in medical, pharmaceutical, cosmetic, and biotechnological products and as a drug carrier [5,48,50].

TG analysis of chitin shows that the weight loss takes place at a temperature of 260 ^{o}C due to cleavage of the C-O-C bonds in the polymer chains. At the temperature of 360 ^{o}C, most of the sample was degraded into a charred material residue [26,64,65,67]. The decomposition takes place in two stages. In the beginning, at a temperature of 50-140 ^{o}C, capillary water accumulated in the micropores of the material evaporates. The presence of micropores makes chitin hygroscopic like other natural polymers. In the second main step, at a temperature of 320-410 ^{o}C, depolymerization, ring dehydration, and functional group decomposition take place [5,28,48,49,69]. At a temperature of 400 ^{o}C, 85 % of the sample decomposes. The main products of the thermal decomposition of chitin are acetamide and acetic acid [70]. The high temperature at which chitin decomposition begins is influenced by its crystal structure. Comparing all 3 chitin crystal structures, it can be seen that α-chitin has inter- as well as intramolecular hydrogen bonds, making it a rigid crystal structure, and its thermal decomposition takes place at the temperature of 330 ^{o}C. β-chitin has weak intermolecular forces. Therefore, its decomposition temperature is the lowest and equals 230 ^{o}C. Gamma chitin has a parallel and antiparallel structure; therefore, its thermal degradation is between the peaks for α and β chitin (around 310 ^{o}C) [26,50]. TGA evaluation of chitins from various sources in thermo oxidative conditions is shown in Figure 4.

In the literature [71,72], there are also studies of chitin thermostability, in which various mathematical models were used, e.g., the iso-conversional procedure of Kissinger – Akahira - Sunose (KAS), which is recommended by the ICTAC committee. The KAS model is used in non - isothermal experiments. According to it, the heating rate does not affect the reaction mechanism for the adopted degree of conversion α. Kissinger – Akahira – Sunose proposed a new linear equation (1):

$$\ln\left(\frac{q}{T^2}\right) = ln\left[\frac{AR}{g(\alpha)E}\right] - \frac{E}{RT} \qquad (1)$$

q- linear constant heating rate

T – temperature

A – preexponential factor

E – activation energy

g(α) – reaction model

For each conversion rate, if the reaction model is known, a line plot ln(q/T2) versus 1/T can be plotted, and E and ln[AR/g(α)E] can be determined from the slope and intersection, which allows us to calculate the factor A [71-73]. This model also allows for predicting lifetimes and preservation of the activation energy of degradation processes when the reaction model is unknown [72,73].

The first degree of chitin degradation at around 100 °C is related to the vaporization of absorbed water. The second stage of decomposition takes place in the range of 235-510 °C and

is related to the evaporation and combustion of volatile compounds. As a result of the pyrolysis of the polysaccharide, acetic and butyric acid and other C2, C3, and C6 fatty acids are formed. At temperatures above 380 °C, the degradation mechanism is likely to change (the g(α)-function will also change), evidenced by two exothermic peaks. The first (up to 380 °C) is associated with the depolymerization of chitin and the formation of volatile products that burn in an oxidizing atmosphere. In comparison, the second (around 453 °C) is associated with the degradation of the formed char [71,72].

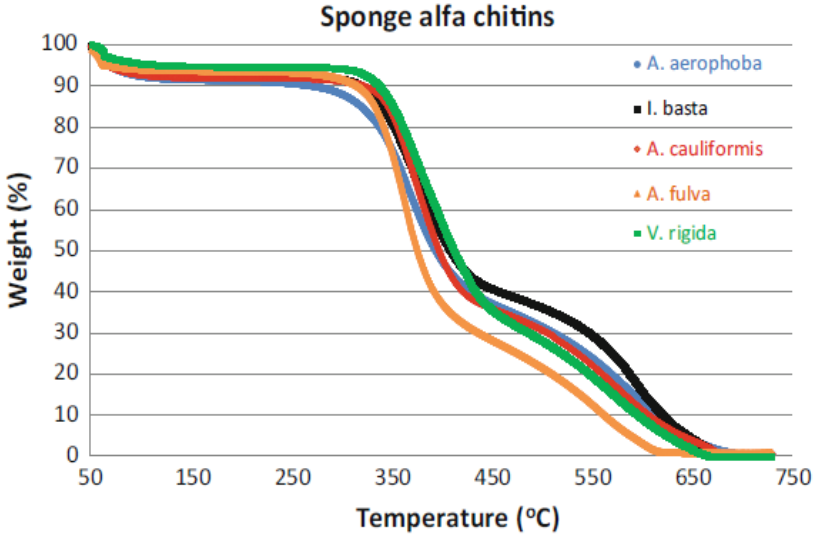

Figure 4. TGA curves of α-chitins (thermo oxidative conditions) [5]. Reprinted by permission from [Springer Nature Customer Service Centre GmbH]: Springer Nature [Extreme biomimetics] (Editor: Hermann Ehrlich) [Chapter 7: Thermogravimetric Analysis of Sponge Chitins in Thermooxidative Conditions] by Dawid Stawski [COPYRIGHT] (2017).

Due to its thermostability [74], recently, chitin has found applications within extreme biomimetics approaches. Biomimetic synthesis offers great opportunities for the development of many innovative biomaterials with unique properties for their implementation in tissue engineering, biomedicine, catalysis, electronics, etc. [75], e.g., the use of marine sponge α-chitin scaffolds as a matrix for the production of zirconium dioxide nanophase from ammonium zirconium (IV) carbonate using hydrothermal synthesis under extreme conditions (150 °C) in order to use the resulting composites for bone and tooth repair and in catalysis [75–77]; the use of β-chitin scaffolds obtained from marine cephalopods as matrices for the production of zinc oxide by the hydrothermal method at a temperature of 70 °C in order to use the resulting composites in dressing materials due to their antibacterial properties [72,75]; the use of α-chitin scaffolds in the synthesis of chitin - silicon composite materials because of chitin silicification at 120 °C for their use in tissue engineering and for the supply of medication [75,79,80]. Chitin of poriferan origin has been used as a template for producing 3D chitin-Fe_2O_3 composites by hydrothermal synthesis at 90 °C and pH 1,5 for their use in electrochemical capacitors [81]. Also, chitin of poriferan origin was used for the hydrothermal synthesis of chitin - germanium oxide nanocomposite at 185 °C, which exhibits specific physical properties, such as a strong enhancement of photoluminescence [82]. Recently, the production of multiphase structural materials based on sponge chitin (chitin-$(Ti/Zr)O_2$) under hydrothermal conditions (160 °C), which show photoluminescent and photocatalytic properties, has been reported, too [80,83]. The available scientific research shows great opportunities for the development of chitinous materials due to their resistance during hydrothermal processes. Microscopic studies show that chitin and fungi with chitin cell walls do not degrade even at temperatures above 200 °C. Only

placing a sample of chitin or fungi with chitin cell walls in supercritical water (p = 25 MPa) and heating it above 380 °C caused chitin degradation [73]. Wysokowski and co-workers [84] reported the deposition of calcium carbonate on matrices derived from marine sponges of *Verongiida* order due to biomineralization using the hemolymph of mollusks (e.g., snails) for the use of the obtained products in tissue engineering.

Chitin-based 3D composite materials with metallic or oxide structures on the surface can also be produced by alternative methods such as electrochemical deposition and coating. Bioelectrometallurgy is one of the directions of extreme biomimetics. Using this approach, chitin can be metalized with copper and copper oxide at room temperature [85]. One of the new methods of isolating chitin from the sponge skeleton is microwave irradiation with following treatment with sodium hydroxide, acetic acid, and hydrogen peroxide. As a result of this treatment, chitin was not deacetylated to chitosan, and its structure was not destroyed. Moreover, all the properties necessary for the use of such ready–to–use 3D scaffolds in biomedicine are retained. Thanks to this method, it is possible to simultaneously produce naturally pre - fabricated 3D composites containing chitin as well as bioactive bromotyrosines [58,86]. Microwave-assisted demineralization allows the quick extraction of chitin without the use of aggressive chemicals (ready–to–use 3D chitin scaffolds are created in order to apply them in biomedicine and technology) [87].

3.3. Chitosan.

Chitosan is a biopolymer obtained by deacetylating chitin in an alkaline environment [88]. It remains to be in the focus of intensive investigations due to diverse structural and physicochemical features as well as biodegradability, biocompatibility, anti-inflammatory, antimicrobial, antifungal, antioxidant, anticancer and wound healing properties [89]. It is a hydrophilic cationic polymer due to the presence of polar groups. Because of the fact that chitosan is also a structural polysaccharide, large amounts of carbon residues are formed as a result of its thermal decomposition [90–92]. As a result of incomplete chitin deacetylation (70-80 %), chitosans can be obtained. Due to their properties, which depend on the degree of deacetylation and crystallinity, they are widely used in industry, agriculture, and medicine, as well as in biocatalysis and drug delivery, mainly due to their cationic nature [28,89,91,82]. A large number of hydrophilic groups and chemically active amino groups, as well as the flexibility of the polymer chain, make chitosans able to coordinate metal ions. In addition, they are easy to obtain from renewable and natural sources, so they are used for wastewater treatment (also for removing metal ions from wastewater) [49,93]. Using the thermal analysis of chitosan [94], it is possible to predict the range of applications of this biomaterial, e.g., the thermal behavior of biosorbents in the process of disposal of heavy metals from sewage [28,82]. Due to the presence of amino groups, chitosan is considered to be the most promising N-doped carbon precursor for energy applications [95].

The thermal stability of chitosan has been the focus of several reports [96–99]. DSC and TGA analysis of chitosan show 3 stages of thermal degradation of this material. The first takes place at a temperature of 30-150 °C and concerns the evaporation of adsorbed water. Then, in the range of 100-170 °C, strongly bound water molecules are released [90]. In the third stage, the degradation of chitosan occurs in the temperature interval 230-400 °C - there is thermal degradation of the polymer chain and evaporation of volatile components [90–93,95,100,101]. At the temperature of 750 °C, most of the sample is degraded. Water, carbon monoxide, carbon dioxide, ammonia, and acetic acid are released during thermal

decomposition. At temperatures above 450 °C, methane is released [95,102]. An analysis conducted in the air atmosphere provides additional information. Water evaporation takes place here already below 50 °C, while the second and third decomposition stages are similar to those taking place in an inert atmosphere. The greatest difference is above 400 °C, where the fourth stage of degradation is visible (in the air atmosphere). Strong oxidation takes place here, followed by thermal decomposition of the oxidized chitosan. This significantly increases the degradation efficiency, as only 4 % of carbon residues remain at the temperature of 600 °C. As much as 35 % of the sample remained in the analysis under a nitrogen atmosphere [90,91]. The comparison of temperatures for individual stages of thermal degradation of chitosan in air and nitrogen atmosphere is presented in Table 2. Comparing the thermal degradation paths of chitosan and its precursor - chitin, it can be seen that the thermal stability of chitosan is lower. This is due to the high degree of deacetylation of chitosan, which also reduces its crystal order [28,49].

Table 2. The comparison of temperatures for individual stages of thermal degradation of chitosan in air and nitrogen atmosphere (based on [90–93,95,100,101]).

	In nitrogen	**In air**
I step	below 100 °C	below 50 °C
II step	100-170 °C	about 180 °C
III step	230-400 °C	220-360 °C
IV step	———	above 400 °C

The thermal stability of chitosan opens the key way to its applications in a broad variety of hydrothermal reactions [103]. Also, chitosan-assisted hydrothermal synthesis of diverse nanostructured composite materials has been reported [104–109].

3.4. Spongin.

Spongin is a structural, fibrous biopolymer of poriferan origin (mostly bath sponges) similar to collagen and keratin. It occurs as the backbone of some marine sponges and is thermostable to around 300 °C [110,111]. The literature shows that spongin is not a pure protein but a biocomposite that also contains xylose, mineral phases, collagen structures, and halogens (I, Br) [5,21]. Its chemical and thermal properties are similar to keratin, e.g., it is resistant to gentle hydrolysis and enzymatic treatment [112,113]. There are comparisons of the structure and chemical composition of keratinized fibers of sponges for silk in the literature. The difference is that the spongin contains iodine, making it useful in pharmacology. The chemical formula for spongin has even been proposed: 20 ($C_{39}H_{62}N_{12}O_{17}$) + $I_2S_3P_{10}$. The presence of halogens in the composition of the spongin makes it highly resistant to enzymatic treatment [114]. It is used in extreme biomimetics as a renewable biomaterial with a natural 3D scaffold architecture. Its use in the immobilization of enzymes, biomedicine, and tissue engineering is also well recognized today [5,80,110,114–116]. An example is the recently reported development of a new 3D spongin - atacamite composite material, which is used in the construction of sensors, catalysts, and antibacterial filters [21]. Spongin is also used as a support for the immobilization of dyes (studies available in the literature confirm that this biomaterial is a good catalyst carrier) [115]. Sponge skeletons are also valued for their unique mechanical properties, i.e., porosity, flexibility, compressibility, absorbency, and durability of the 3D structure [113,115]. The properties and thermostability of spongin open up many new possibilities for developing new composite materials with the use of hydrothermal synthesis. The materials obtained in this way have a hierarchical and nano-structured organization and a

3D architecture on macro - levels and micro - levels. 3D scaffold (Figure 5) is isolated from marine demosponges, such as *Hippospongia communis* - their marine farming is found all over the world [111,112,114,117]. The spongin's particularly noteworthy properties are nanofibers' hierarchical structure and the triple helix's collagen structure - all these features are retained even after pyrolysis up to 1200 ^{o}C [19,80].

Figure 5. Spongin-based 3D scaffold isolated from *H. communis* demosponge.

The literature provides research on the transformation of a sponge skeleton into carbon at high temperatures without destroying its structure - as a result of the appearance of nanopores, the specific surface of the carbon increases, which favors its further processing towards using it as a catalyst [19,112,118]. In order to ensure optimal carbonization conditions, it is necessary to know the kinetics of the thermal decomposition of the spongin. Moreover, the available research proves that the heat treatment temperature increases the structure of the obtained carbon materials [118]. There are also studies on the carbonization of the sponge skeleton at a temperature of 1200 ^{o}C, resulting in a 3D turbostratic graphite that retains all the nanostructural features characteristic of the collagen triple helix. Then the resulting composite is galvanized with copper to obtain a hybrid (Cu/Cu_2O) with unique catalytic properties, i.e., reduction of p-nitrophenol in an aqueous medium. This example shows the potential of extreme biomimetics in the progress of new composite materials. The copper hybrid obtained here is used in environmental protection [19].

The use of sponge skeletons to immobilize enzymes, including laccase, is also of scientific interest. Such systems are used to degrade hazardous compounds: bisphenol A, bisphenol F, and bisphenol S. As a result, phenolic impurities can be removed from wastewater using environmentally friendly methods. Due to the immobilization of laccase, the possibility of its reuse has been increased [119,120]. Sponge scaffolds also adsorb dyes, e.g., anthocyanins. The resulting hybrid material shows antioxidant properties and is able to remove up to 95 % of free radicals from the solution, which has been proven in the literature. Such a material shows much better thermostability than the dye itself [121]. Another natural dye that adsorbs on the spongin-based skeletons of demosponges is carmine (cochineal). Like other dyes, adsorption causes electrostatic interactions and hydrogen bonds between the dye and the sponge skeleton - it makes the thermostability of hybrid materials better than pure spongin. Such hybrid material finds application in drug delivery systems [117]. There are also studies

available in the literature on the adsorption of sodium - copper chlorophyllin on the demosponge sponginess skeleton - such a hybrid material has an antibacterial effect against Gram-positive bacteria. The TG analysis of such a hybrid material shows that the greater the amount of adsorbed chlorophyllin, the better the thermal stability of the material (the thermostability of the hybrid is better than that of pure spongin) [116].

In modern materials science, nanostructured composites are obtained using extreme biomimetics, e.g., a MnO_2-based composite made with a carbonized spongin. Such a composite has much better electrochemical properties than manganese dioxide, due to which it is used in the storage and processing of energy from renewable sources [113,122]. In this way, a magnetic 3D sponge scaffold with Fe_3O_4 nanocores was also obtained [110]. This composite has been used to remove cationic dyes, i.e., crystal violet and methylene blue, proving that it has good absorption capacity. As a result, it can be used for wastewater treatment as an ecological adsorbent and drug delivery.

Moreover, the magnetic composite exhibits much better thermal stability than pure spongin [110]. A hematite-based composite can also be obtained from spongin by hydrothermal synthesis commonly used in extreme biomimetics. Such a hematite-spongin composite has been used as an anode material in capacitors because it positively affects the capacity of energy stores and its thermal stability is comparable to pure spongin. Another important application of sponge scaffolds is biocatalysis, e.g., during the transesterification of canola oil using methanol in the production of biofuels. For this purpose, lipase B is immobilized on 3D sponge scaffolds. As a result, lipase has better thermal and chemical stability. Its catalytic activity is maintained in a wide range of temperatures and pH, and it is possible to use it multiple times [123]. The above examples show that spongin, because of its high thermal stability, can be used to produce new composite materials with unique properties for use in biomedicine, electronics, biotechnology, catalysis, and nanotechnology [113,124].

Studies of spongin structures isolated from diverse marine sponges are available in the literature. Such biomaterials are used to produce 2D films for wound dressings and tissue regeneration. This is mainly due to high mechanical and thermal resistance, biocompatibility, and antioxidant properties [125].

From the analysis of the thermal degradation of spongin, the first degree of weight loss can be seen at 80-150 ^oC. It is caused by the evaporation of water from the sponge skeleton. The second degree of degradation occurs in the range of 200-420 ^oC and is associated with the degradation of the protein matrix - breaking of peptide bonds and thermal degradation of disulfide bridges and hydrogen bonds [111,112,117,118,126]. At a temperature of 1000 ^oC, the spongin sample is about 77 % degraded [108,114]. During thermal degradation of spongin, many gaseous products are formed, e.g., water, carbon dioxide, ammonia, nitrogen oxides, sulfur dioxide, hydrogen sulfide, and short-chain alkenes [118]. The literature also provides tests of the thermal stability of spongin-based materials, e.g., materials functionalized with silver or cobalt groups. As a result of the control of the thermal movement of the biopolymer matrix, they significantly increase the thermal stability of the material compared to pure spongin [112].

3.5. Collagen.

Collagen is a structural protein with alternating hydrophilic and hydrophobic zones in the polypeptide chain and creates a triple helix structure [127,128]. Collagen is the main component of the skin; it is also found in connective tissue, where its fibrous structure protects

against mechanical damage. It also plays a crucial role in the biomineralization of both vertebrates [6,129,130] and invertebrates [4,131,132]. Currently, this biopolymer is widely used in medicine, the cosmetics industry, and the production of leather and fur products [127,133]. Due to its very good biocompatibility, collagen is used in tissue engineering [134] after modification to improve its physicochemical properties - unprocessed collagen has low stability and poor mechanical strength [133,135–137]. The most common form of collagen is collagen I, used mainly in the pharmaceutical, food, and biomedicine industries. It has very good mechanical properties but is easily subject to thermal degradation, limiting its possible applications [138].

The thermal stability of collagen depends on the source from which it was obtained. Collagen isolated from fish has lower thermostability than mammalian collagen, which limits its use and may be related to the living environment and the content of imino acids, i.e., proline and hydroxyproline. Collagen thermostability varies between 15 °C and 40 °C depending on its source [137]. Collagen is another natural biopolymer with great potential for biomedical applications as a biomaterial, which is why many studies are conducted on its chemical modification to improve its low thermal stability [138–140], limiting its use. Native collagen is poorly soluble in water. Therefore, modifiers are used to lower the isoelectric point. Also, its denaturation takes place at a temperature below 40 °C. Therefore, in order to increase its thermostability, physical modifications are made, e.g., UV radiation, and chemical modifications, e.g., glutaraldehyde, formaldehyde, hexamethylene diisocyanate [141]. The low thermostability of collagen is an obstacle in using this biopolymer, e.g., for the manufacture of packages in the food sector. Studies aimed at improving collagen's thermal stability and mechanical properties are available in the literature. For this purpose, collagen cross-linking is carried out with proteins of high thermostability, i.e., casein, keratin, and soy protein isolate. The obtained protein complexes show better thermal stability, tensile strength, and elongation at break. The best effect was obtained with casein after collagen cross-linking with the use of transglutaminase as the catalyst of the reaction. In the case of collagen, the peak temperature is 82 °C, and the collagen-casein complex cross-linked with transglutamate increased to 130 °C [138].

Depending on the source, collagen differs in molecular weight and the temperature at which individual stages of thermal degradation occur (it differs in thermostability). However, for all samples, there are 3 stages of thermal decomposition. The hydrogen bonds are broken in the first one, and the water evaporates. In the second stage, the weight loss of the sample is significant. It results from breaking the bonds in collagen, decarboxylation, and the formation of gaseous decomposition products, i.e., carbon dioxide, carbon monoxide, ammonia [127,135,137,142]. In the third stage, almost complete degradation of the sample occurs - at a temperature of 800 °C, over 97 % of the sample is degraded [127,143]. Table 3 shows the temperatures at which the greatest weight loss occurs during the various steps of thermal degradation using the example of native collagen.

Table 3. Temperatures at which maximum weight losses occurred in air atmosphere for native collagen (based on [143]).

	Temperature
I step	111 ºC
II step	308 ºC
III step	570 ºC

3.6. Keratin.

Keratin is a structural protein that occurs naturally in hair, feathers, wool, and nails. Keratin is produced by the epidermis cells and protects the skin [144]. Keratin is also found in diverse marine organisms. Intermediate fibers are a component of the cytoskeleton and are the fibrous components of α-keratins, e.g., skin, hair, and nails, but are also found in living cells. From intermediate fibers, animals construct many different biomaterials with unique mechanical properties. These fibers are distributed mainly inside the cells, but in hagfish, they are secreted as mucus in stressful situations [145]. This biopolymer has very good mechanical properties because of the high degree of disulfide cross-links, hydrogen bonds, and hydrophobic effects [146–148]. The presence of disulfide bridges between cysteine residues contributes to the high thermostability of keratin [147,149,150]. The temperatures of keratin denaturation vary slightly depending on its source [151]. Still, the keratin found in the hair is the most persistent because its non-helical domains contain the most cysteine residues [5]. Keratin-based materials can be used in biomedicine, biotechnology, and tissue engineering due to their biodegradability and biocompatibility [152,153]. Keratin does not dissolve in water, but as a result of the research carried out, it was found that it dissolves well in ionic liquids. The use of keratin is becoming more and more common due to the development of efficient keratin extraction methods that do not cause significant deformation of the secondary structure of this fibrous protein [148,154].

There are three main stages in the thermal decomposition of keratin, in which there is a significant loss of mass of the sample. The first takes place at a temperature below 200 °C and is caused by the vaporization of water. The next stage takes place in the range of 200-400 °C and is caused by the degradation of organized structures, and keratin matrix - volatile compounds such as carbon monoxide, carbon dioxide, ammonia, hydrogen sulfide, sulfur dioxide, methane, and hydrogen cyanide are released (sulfur compounds are released due to cleavage of the disulfide bond of the cysteine residue) [144,146,148,149,155–158]. The third step is in the range of 410-650 °C, and the total weight loss of the sample after this step is 95,5 % [144]. The DCS analysis available in the literature shows that the temperature range over which cysteine degradation occurs is consistent with the temperature range over which the crystal transition (melting) occurs. These two processes are related to each other because cysteine residues greatly influence the thermostability of the keratin fibers. Breaking the disulfide bonds makes the fibers more susceptible to heat and weakens the conformation of the protein, leading to partial melting [159]. The high thermal stability of keratin compared to other biopolymers, e.g., collagen is a great advantage - it allows the creation of new materials with several different industrial and biomedical applications [150]. The literature presents studies of the thermal stability of feather keratin to produce new thermosetting composites based on spun-bonded nonwovens with the addition of feather keratin. Studies have shown that nonwoven based on polylactide/chicken feathers exhibit much greater tensile strength and better thermal stability than keratin [148].

3.7. Silk.

Silk is a natural fibrous protein produced mostly by silkworms, scorpions, spiders, mites, and marine amphipods [160]. The silk fibers are composed of sub-fibers, the core of which is fibroin. Silk fibers mainly consist of fibroin and sericin - a protein referred to as glue, and are stable up to around 140 °C. Sericin-containing silk exists as a random coil or as an α-

helix structure, while silk without sericin appears as a β-sheet structure (the silk β-sheet structure is much more stable than the triple helix in collagen) [161,162]. Due to their properties, i.e., non-toxicity, biocompatibility, and biodegradability, silk-based materials can be used in biomedicine as medical materials, cosmetics, biotechnology, and food additives [163–165]. Silk fibers are also characterized by high strength and ductility due to the high-order structure. In addition to natural silk, there are also materials based on regenerated silk, composite materials, and chemically synthesized artificial materials, e.g., by polymerization [166]. Studies of the influence of cosmic rays on the structure and stability of silk-based materials are available in the literature. They are very important in the context of designing a new generation of biomaterials used in the space environment. These studies showed that 15 % of the surface was digested by ionizing molecules, e.g., atomic oxygen, and 80 % of the material was cross-linked with cosmic rays [162].

Spider silk is used in biomimetic research due to its many desirable characteristics [167,168]. As a result of the shrinkage of silk fibers, significant stresses are generated after wetting, which can be used in industry, mainly in robotics and various types of sensors [169]. Furthermore, through the chemical alteration of silk fibers, materials with better properties can be obtained [170], which will significantly expand the scope of their potential applications, e.g., the presence of siloxane bonds results in better thermal stability and resistance to oxidation and water resistance [171].

The first stage of thermal decomposition of silk occurs at a temperature below 100 °C and is related to the vaporization of water [172–174]. The main stage of thermal degradation takes place in the range of 310-480 °C due to the breakdown of side-chain groups of silk fibroin. The last significant weight loss occurs in the range of 500-650 °C due to the breakdown of main chain groups of silk fibroin. In the literature, thermogravimetric tests of silk containing sericin and without this protein are available. It is worth noting that the sericin present in silk slightly reduces the thermal stability of silk [172,174–176]. At a temperature of 600 °C, about 70 % of the sample is degraded [177]. Studies comparing the thermal decomposition of silk in nitrogen, air, and oxygen atmosphere are also available.

The degradation of the sample in oxygen is the fastest, and in nitrogen - the slowest [178]. Thermogravimetric analysis of silk samples from outer space showed that their thermal stability decreased - at a temperature of up to 120 °C they lost about 40 % of their mass [162]. The literature also compares the thermal stability of silk obtained from various sources, e.g., cocoons and fibrous waste. These samples differ slightly in thermal properties, and additional treatment by annealing with water increased the glass transition temperature of the samples. The presence of a crystalline structure in the samples depends on the raw material and the treatment method. These studies are aimed at showing alternative methods of obtaining and processing silk in order to be able to control the structure and properties of the material [179]. The literature also describes the influence of water on the thermal stability of silk samples. Increasing the amount of water in the silk sample does not affect the material's thermal stability but increases the amount of free water that is removed at a lower temperature and lowers the glass transition temperature. Understanding the effect of water content on silk's thermal stability is critical to its use in construction materials [174]. The influence of temperature on conformational changes of both raw and processed silk fibers is also described in the literature. The elevated temperature causes the transition from the β-sheets structures to the β-turns. These tests aim to control the structure of the produced silk-based materials [180]. The available results of studies on the increase in crystallinity in silk fibroin are also interesting. This

biopolymer is obtained from silk fibrous waste (cheaply obtained from natural sources), which means that it contains a lot of amorphous structures that cause good water solubility, limiting its use in biomedicine. The research results prove that treatment in ethyl alcohol, especially in methyl alcohol, causes the growth of crystal structures in the sample, which creates favorable conditions for the use of this material in biomedicine. The increase in crystallinity also improves the material's thermal stability, causes an increase in the glass transition temperature, and decreases water absorption rates [181].

3.8. Byssus.

Byssus is a structural protein of molluscan origin whose fibers have an amino acid composition similar to collagen [182]. The polar or hydrophobic side chains of these amino acids are more elaborate than those of silk. It occurs in some mollusks, e.g., mussels. Byssus has a low degree of molecular orientation. It is heat resistant, just like silk. The literature describes that collagen is the main component of byssus fibers [183–186]. Byssus consists of two parts: rigid distal and flexible proximal. Each of them contains a specific type of collagen protein [4,184,187]. The distal threads take up about 80 % of the total length of the byssus and determine its extensibility and hardness [186,188]. It is assumed that the strength of byssus is six times greater than that of collagen contained in human tendons and is comparable to carbon fibers and Kevlar [187]. The properties of byssus fibers depend on the water content - dry fibers show elastoplastic behavior, while wet fibers are similar to elastomers. Due to the unique mechanical, thermal, and adhesive properties of byssus, it has a number of different applications. It can be used in dental and surgical adhesives, biosensors, tissue engineering, biomimetics, and biotechnology [4,187]. Byssus is the most sticky protein - wet adhesion in mussels is possible due to the presence of 3,4-dihydroxyphenylalanine (DOPA). The adhesive ability by adhesion can be used in biomimetics, but the problem is the spontaneous oxidation of DOPA. Therefore, it is important to control the DOPA redox reaction - the oxidized form shows cohesion and reduced adhesion. Such control exists in mussels because they have the so-called probe, a free radical diphenylpicrylhydrazyl (DPPH). Understanding redox control will allow the development of novel adhesive polymers [189–191]. There are also studies on the design of synthetic materials made of byssus in the literature. The development of research techniques makes it possible to trace selected proteins during the formation of strands from soluble precursors to solid fibers. Protein precursors spontaneously organize into complex architectures, and maturation takes place in subsequent regulated steps. This research allows using the unique properties of byssus, i.e., wet adhesion and self-healing ability, to produce new materials for biomedical and industrial applications [190]. The production of byssus-based materials focuses on using metal coordination chemistry mediated by histidine and DOPA to produce wet adhesives and self-healing materials. However, this is a minimalist action, as the complexity of byssus proteins is reduced to single amino acid groups. Intensive work is underway on biotechnological methods to obtain innovative materials based on byssus, using its unique properties and complexity of the structure, which will allow the structure and properties of the produced materials to be controlled in order to be used in industry and the production of construction materials. Biotechnological methods consist in the production of materials from purified proteins, recombinant proteins, and synthetic peptides. Modern methods of producing byssus-based materials in line with the principles of biomimetics also include emulsion-based drops that contain polymer precursor reagents. Thanks to them, it is

possible to produce materials with a hierarchical structure, heterogeneous composition, and unique properties, such as self-healing ability [186,191].

Thermal analysis shows a slight decrease in the weight of the sample up to 200 ^{o}C due to water evaporation. In the range of 230-320 °C, there is a greater mass loss due to the decomposition of the ordered structure and thermal decomposition of collagen fibers of byssus (similar to collagen, where at 217 °C, the structure degradation begins). The thermal behavior of byssus resembles that of silk fibers (main thermal decomposition above 300 °C), despite the different amino acid composition and conformation of these two biopolymers [183,184,187,188]. In the range of 550-600 ^{o}C, there is also a significant loss of sample mass, which is related to the degradation of the organic matrix and byssus proteins [188]. At a temperature of 900 ^{o}C, the sample weight of byssus is reduced by 70 % [184].

3.9. Conchiolin.

Conchiolin is an aggregate of proteins that contains a large proportion of the polysaccharide component. This structural protein is found in the tissues of mollusks. Conchiolin contains high amounts of glycine and alanine as well as hydrophobic residues. It is insoluble in water and acids. There are domains typical for collagen in the conchiolin; therefore, these proteins may show similar properties. Due to its biocompatibility, conchiolin is used in biomedicine, tissue engineering, wound healing, and bone engineering due to its ability to bind calcium [113,192–194].

Figure 6. Conchiolin-based conchix (yellow) isolated during decalcification of molluscan shell.

The material contained in the shells of mollusks is important in materials science, the cosmetics, pharmaceutical, feed industries, and biotechnology. The shells of mollusks are a waste of seafood consumed all over the world. One method of isolating Conchixes (organic scaffolds) (Figure 6) is demineralizing the shells with EDTA. The isolated material is used for research on the practical application of mollusk shells in the production of modern biomaterials [195].

There are few studies on the thermostability of conchiolin, but in the literature, we can find information that the conchiolin sample was pyrolyzed at temperatures up to 900 ^{o}C. Polypeptide assemblies were still present in the samples after pyrolysis, proving a very high

resistance of conchiolin to pyrolysis [193,194,196,197]. The thermostability of conchiolin and other reviewed natural polymers is summarized in Table 4.

Table 4. Thermostability characteristics of the reviewed natural biopolymers.

Biomaterial	Temperature of the first stage of degradation	Temperature of the second stage of degradation	Temperature of the third stage of degradation	Temperature of the fourth stage of degradation	References
Cellulose	below 100 °C (in nitrogen and air)	400 °C (in nitrogen) and 360 °C (in air)	475 °C in air	———	[25,31-33,35,41,42]
Chitin	50-140 °C	235-510 °C	———	———	[5,28,48,49,69,71,72]
Chitosan	below 100 °C (in nitrogen) and below 50 °C (in air)	100-170 °C (in nitrogen) and 180 °C (in air)	230-400 °C (in nitrogen) and 220-360 °C (in air)	above 400 °C in air	[90-93,95,100,101]
Spongin	80-150 °C	200-420 °C	———	———	[111,112,117,118,126]
Collagen (native)	111 °C	308 °C	570 °C	———	[127,135,137,142,143]
Keratin	below 200 °C	200-400 °C	410-650 °C	———	[144,146,148,149, 155-158]
Silk	below 100 °C	310-480 °C	500-650 °C	———	[172-174,177]
Byssus	up to 200 °C	230-320 °C	above 300 °C	550-600 °C	[183,184,187,188]
Conchiolin	pyrolysed up to 900 °C				[193,194,196,197]

4. Conclusions

The renewable biological materials presented in this review can be used to develop new biocomposites with unique mechanical and physicochemical properties. Using nature's resources as a tool for materials science balances obtaining new materials with desired properties and maintaining low toxicity, biocompatibility, biodegradability, and ecofriendly approach. However, thermostability is a key parameter that must be considered in conducted research, especially due to big progress in extreme biomimetics and the development of a new generation of composite materials. The lowest thermostability of the discussed biopolymers is shown by collagen, which, depending on its origin, can decompose at a temperature 15 °C. The remaining biopolymers show much better thermal stability, which allows for their wide applications. One of the most thermostable biopolymers is spongin, the complete degradation of which takes place only at about 1000 °C. Due to the good thermostability of the described biopolymers, it is possible to produce a wide range of new materials with previously unknown properties using modern methods, such as hydrothermal synthesis. Such materials are used in many fields, i.e., biomedicine, biotechnology, pharmaceuticals, tissue engineering, catalysis, nanotechnology, and others. When selecting biological materials, it is also critical to understand their origin and the presence of potential contaminants, which will directly affect the mechanism of thermal degradation. It is extremely important to know the thermal stability of materials, both in terms of ongoing synthesis and potential applications. In particular, the next major step in the studies should be large-scale research in various science disciplines, for example, for medical, pharmaceutical, or biotechnological issues.

5. Outlook

The biopolymers presented in this review are naturally occurring and renewable compounds. Therefore, research into the development of methods for their use in the production of modern materials is a very important trend in the further progress of materials science. The extreme biomimetics approach will allow the use of all physical, chemical,

mechanical, thermal, and structural properties of these biopolymers to produce ecological and innovative materials with many potential applications and which can be an alternative to harmful and environmentally polluting artificial polymers. The knowledge of the thermostability of each of the biopolymers is crucial for the appropriate selection of methods for its modification, increasing thermal stability, and an indication of potential applications. As a result of the high thermostability of the materials discussed in this review, it is possible to use modern methods of biopolymer modification, such as hydrothermal synthesis. The development of extreme biomimetics in the production of materials based on the biopolymers discussed in this review creates many opportunities for their application, mainly in areas such as biomedicine, biotechnology, pharmaceuticals, tissue engineering, broadly understood industry (including construction materials, food additives), catalysis, electronics, nanotechnology and many more. As one of the most thermally stable biopolymers discussed in this review, spongin offers many opportunities to produce new biocomposites because the 3D structure is not damaged at extremely high temperatures. Moreover, the production of byssus-based materials, which has unique adhesive properties, is still underdeveloped, as is the case of conchiolin, where research on its thermostability and the production of new materials based on it are still poorly described in the literature. The development of the chemistry of materials based on these biopolymers may contribute to the creation of unique materials with previously unknown properties and many possibilities for their potential practical application in the future.

Funding

This research was funded by the National Science Centre within the framework of the project Maestro No. 2020/38/A/ST5/00151.

Acknowledgments

This review has no acknowledgments.

Conflicts of Interest

The authors declare no conflict of interest.

References

1. Ehrlich, H. Marine Biological Materials of Invertebrate Origin. 1st ed. Springer **2019**, https://doi.org/10.1007/978-3-319-92483-0.
2. Park, J.; Lakes, R.S. Biomaterials: An Introduction. 3rd ed. Springer, **2007**, https://doi.org/10.1007/978-0-387-37880-0.
3. Leali, P.T.; Merolli, A. Fundamentals of Biomaterials. In Biomaterials in Hand Surgery. Merolli, A.; Joyce, T.J. Springer-Verlag, Milano, **2009**, pp. 1–11, https://doi.org/10.1007/978-88-470-1195-3.
4. Ehrlich, H. Biological Materials of Marine Origin. Invertebrates. Springer **2010**, https://doi.org/10.1007/978-90-481-9130-7.
5. Stawski, D. Thermogravimetric Analysis of Sponge Chitins in Thermooxidative Conditions. In Extreme biomimetics; Ehrlich, H. Eds.; Springer, Cham. **2017**, pp. 191-203, https://doi.org/10.1007/978-3-319-45340-8_7.
6. Ehrlich, H. Biological Materials of Marine Origin. Vertebrates. 1st ed.; Springer **2015**, https://doi.org/10.1007/978-94-007-5730-1.
7. Gil, E.S.; Park, S.H.; Hu, X.; Cebe, P.; Kaplan, D.L. Impact of sterilization on the enzymatic degradation and mechanical properties of silk biomaterials. *Macromol. Biosci.* **2014**, *14*, 257–269, https://doi.org/10.1002/mabi.201300321.

8. Lucke, M.; Winter, G.; Engert, J. The effect of steam sterilization on recombinant spider silk particles. *Int. J. Pharm.* **2015**, *481*, 125–131, https://doi.org/10.1016/j.ijpharm.2015.01.024.
9. Rogers, W.J. Steam and dry heat sterilization of biomaterials and medical devices. *Sterilisation Biomater. Med. Devices* **2012**, 20–55, https://doi.org/10.1533/9780857096265.20.
10. Zhou, Q.; Malm, E.; Nilsson, H.; Larsson, P.T.; Iversen, T.; Berglund, L.A.; Bulone, V. Nanostructured biocomposites based on bacterial cellulosic nanofibers compartmentalized by a soft hydroxyethylcellulose matrix coating. *Soft Matter* **2009**, *5*, 4124–4130, https://doi.org/10.1039/b907838j.
11. Kaplan, D.L. Biopolymers from Renewable Resources. 1st ed. Springer-Verlag, **1998**, https://doi.org/10.1007/978-3-662-03680-8.
12. Elices, M. Structural Biological Materials: Design and Structure-Property Relationships. 1st ed. Pergamon, **2000**, pp. 1-17, 221-335, https://doi.org/10.1016/s1470-1804%2800%29x8001-7.
13. Meyers, M.A.; Lin, A.Y.M.; Seki, Y.; Chen, P.; Kad, B.K.; Bodde, S. Structural Biological Composites: An Overview. *Biol. Mater. Mech.* **2006**, 35–41, https://doi.org/10.1007/s11837-006-0138-1.
14. Meyers, M.A.; McKittrick, J.; Chen, P.Y. Structural biological materials: Critical mechanics-materials connections. *Science* **2013**, *339*, 773–779, https://doi.org/10.1126/science.1220854.
15. Ehrlich, H. Chitin of Poriferan Origin as a Unique Biological Material. *Blue Biotechnol. Prod. Use Mar. Mol.* **2018**, *2*, 821–854, https://doi.org/10.1002/9783527801718.ch26.
16. Morales, A.; Labidi, J.; Gullón, P.; Astray, G. Synthesis of advanced biobased green materials from renewable biopolymers. *Curr. Opin. Green Sustain. Chem.* **2021**, *29*, https://doi.org/10.1016/j.cogsc.2020.100436.
17. Lazarus, B.S.; Velasco-Hogan, A.; Gómez-del Río, T.; Meyers, M.A.; Jasiuk, I. A review of impact resistant biological and bioinspired materials and structures. *J. Mater. Res. Technol.* **2020**, *9*, 15705–15738, https://doi.org/10.1016/j.jmrt.2020.10.062.
18. Naik, R.R.; Singamaneni, S. Introduction: Bioinspired and Biomimetic Materials. *Chem. Rev.* **2017**, *117*, 12581–12583, https://doi.org/10.1021/acs.chemrev.7b00552.
19. Petrenko, I.; Summers, A.P.; Simon, P.; Żółtowska-Aksamitowska, S.; Motylenko, M.; Schimpf, C.; Rafaja, D.; Roth, F.; Kummer, K.; Brendler, E. Extreme biomimetics: Preservation of molecular detail in centimeter-scale samples of biological meshes laid down by sponges. *Sci. Adv.* **2019**, *5*, 1–12, https://doi.org/10.1126/sciadv.aax2805.
20. Ehrlich, H.; Bailey, E.; Wysokowski, M.; Jesionowski, T. Forced biomineralization: A review. *Biomimetics* **2021**, *6*, 1–30, https://doi.org/10.3390/biomimetics6030046.
21. Tsurkan, D.; Simon, P.; Schimpf, C.; Motylenko, M.; Rafaja, D.; Roth, F.; Inosov, D.S.; Makarova, A.A.; Stepniak, I.; Petrenko, I. Extreme Biomimetics: Designing of the First Nanostructured 3D Spongin–Atacamite Composite and its Application. *Adv. Mater.* **2021**, *33*, https://doi.org/10.1002/adma.202101682.
22. Bischof, J.C.; He, X. Thermal stability of proteins. *Ann. N. Y. Acad. Sci.* **2006**, *1066*, 12–33, https://doi.org/10.1196/annals.1363.003.
23. Gabbott, P. Principles and Applications of Thermal Analysis 1st ed. Blackwell, **2008**, https://doi.org/10.1002/9780470697702.
24. Ramachandran, V.S.; Paroli, R.M.; Beaudoin, J.J.; Delgado, A.H. Handbook of Thermal Analysis of Construction Materials; Noyes Publications/William Andrew Publishing, **2002**, 1-34, https://doi.org/10.1016/S0040-6031(03)00230-2.
25. Cabrales, L.; Abidi, N. On the thermal degradation of cellulose in cotton fibers. *J. Therm. Anal. Calorim.* **2010**, *102*, 485–491, https://doi.org/10.1007/s10973-010-0911-9.
26. Stawski, D.; Rabiej, S.; Herczyńska, L.; Draczyński, Z. Thermogravimetric analysis of chitins of different origin. *J. Therm. Anal. Calorim.* **2008**, *93*, 489–494, https://doi.org/10.1007/s10973-007-8691-6.
27. Ng, H.M.; Saidi, N.M.; Omar, F.S.; Ramesh, K.; Ramesh, S.; Bashir, S. Thermogravimetric Analysis of Polymers. *Encycl. Polym. Sci. Technol.* **2018**, 1–29, https://doi.org/10.1002/0471440264.pst667.
28. Wanjun, T.; Cunxin, W.; Donghua, C. Kinetic studies on the pyrolysis of chitin and chitosan. *Polym. Degrad. Stab.* **2005**, *87*, 389–394, https://doi.org/10.1016/j.polymdegradstab.2004.08.006.
29. Poletto, M.; Ornaghi Júnior, H.L.; Zattera, A.J. Native cellulose: Structure, characterization and thermal properties. *Materials (Basel)* **2014**, *7*, 6105–6119, https://doi.org/10.3390/ma7096105.
30. D'Acierno, F.; Hamad, W.Y.; Michal, C.A.; Maclachlan, M.J. Thermal Degradation of Cellulose Filaments and Nanocrystals. *Biomacromolecules* **2020**, *21*, 3374–3386, https://doi.org/10.1021/acs.biomac.0c00805.
31. Dai, L.; Nan, J.; Tu, X.; He, L.; Wei, B.; Xu, C.; Xu, Y.; Li, S.; Wang, H.; Zhang, J. Improved thermostability and cytocompatibility of bacterial cellulose/collagen composite by collagen fibrillogenesis. *Cellulose* **2019**,

26, 6713–6724, https://doi.org/10.1007/s10570-019-02530-w.
32. Huang, M.R.; Li, X.G. Thermal degradation of cellulose and cellulose esters. *J. Appl. Polym. Sci.* **1998**, *68*, 293–304, https://doi.org/10.1002/(SICI)1097-4628(19980411)68:2<293::AID-APP11>3.0.CO;2-Z.
33. Mamleev, V.; Bourbigot, S.; Yvon, J. Kinetic analysis of the thermal decomposition of cellulose: The main step of mass loss. *J. Anal. Appl. Pyrolysis* **2007**, *80*, 151–165, https://doi.org/10.1016/j.jaap.2007.01.013.
34. Aditya, T.; Allain, J.P.; Jaramillo, C.; Restrepo, A.M. Surface Modification of Bacterial Cellulose for Biomedical Applications. *Int. J. Mol. Sci.* **2022**, *23*, https://doi.org/10.3390/ijms23020610.
35. Henrique, M.A.; Flauzino Neto, W.P.; Silvério, H.A.; Martins, D.F.; Gurgel, L.V.A.; Barud, H. da S.; Morais, L.C. de; Pasquini, D. Kinetic study of the thermal decomposition of cellulose nanocrystals with different polymorphs, cellulose I and II, extracted from different sources and using different types of acids. *Ind. Crops Prod.* **2015**, *76*, 128–140, https://doi.org/10.1016/j.indcrop.2015.06.048.
36. Zhao, G.; Du, J.; Chen, W.; Pan, M.; Chen, D. Preparation and thermostability of cellulose nanocrystals and nanofibrils from two sources of biomass: rice straw and poplar wood. *Cellulose* **2019**, *26*, 8625–8643, https://doi.org/10.1007/s10570-019-02683-8.
37. Wang, D.; Yang, T.; Li, J.; Zhang, J.; Yu, J.; Zhang, X.; Zhang, J. Thermostable and Redispersible Cellulose Nanocrystals with Thixotropic Gelation Behavior by a Facile Desulfation Process. *ACS Sustain. Chem. Eng.* **2020**, *8*, 11737–11746, https://doi.org/10.1021/acssuschemeng.0c03838.
38. Vanderfleet, O.M.; Reid, M.S.; Bras, J.; Heux, L.; Godoy-Vargas, J.; Panga, M.K.R.; Cranston, E.D. Insight into thermal stability of cellulose nanocrystals from new hydrolysis methods with acid blends. *Cellulose* **2019**, *26*, 507–528, https://doi.org/10.1007/s10570-018-2175-7.
39. Santmartí, A.; Lee, K-Y. Crystallinity and Thermal Stability of Nanocellulose. In Nanocellulose and Sustainability, 1st ed.; Lee, K.-Y., Eds.; CRC Press, **2018**, pp. 67-86, https://doi.org/10.1201/9781351262927-5.
40. Sharma, P.R.; Varma, A.J. Thermal stability of cellulose and their nanoparticles: Effect of incremental increases in carboxyl and aldehyde groups. *Carbohydr. Polym.* **2014**, *114*, 339–343, https://doi.org/10.1016/j.carbpol.2014.08.032.
41. Várhegyi, G.; Szabó, P.; Antal, M.J. Kinetics of the thermal decomposition of cellulose under the experimental conditions of thermal analysis. Theoretical extrapolations to high heating rates. *Biomass and Bioenergy* **1994**, *7*, 69–74, https://doi.org/10.1016/0961-9534(95)92631-H.
42. Yang, P.; Kokot, S. Thermal analysis of different cellulosic fabrics. *J. Appl. Polym. Sci.* **1996**, *60*, 1137–1146, https://doi.org/10.1002/(SICI)1097-4628(19960523)60:8<1137::AID-APP6>3.0.CO;2-M.
43. Roman, M.; Winter, W.T. Effect of Sulfate Groups from Sulfuric Acid Hydrolysis on the Thermal Degradation Behavior of Bacterial Cellulose. *Biomacromolecules* **2004**, *5*, 1671–1677, https://doi.org/10.1021/bm034519+.
44. Grønli, M.; Antal, M.J.; Várhegyi, G. A round-robin study of cellulose pyrolysis kinetics by thermogravimetry. *Ind. Eng. Chem. Res.* **1999**, *38*, 2238–2244, https://doi.org/10.1021/ie980601n.
45. Albu, M.G.; Vuluga, Z.; Panaitescu, D.M.; Vuluga, D.M.; Căşărică, A.; Ghiurea, M. Morphology and thermal stability of bacterial cellulose/collagen composites. *Cent. Eur. J. Chem.* **2014**, *12*, 968–975, https://doi.org/10.2478/s11532-014-0545-z.
46. Jusner, P.; Schwaiger, E.; Potthast, A.; Rosenau, T. Thermal stability of cellulose insulation in electrical power transformers – A review. *Carbohydr. Polym.* **2021**, *252*, https://doi.org/10.1016/j.carbpol.2020.117196.
47. Tsurkan, M. V.; Voronkina, A.; Khrunyk, Y.; Wysokowski, M.; Petrenko, I.; Ehrlich, H. Progress in chitin analytics. *Carbohydr. Polym.* **2021**, *252*, https://doi.org/10.1016/j.carbpol.2020.117204.
48. Nam, Y.S.; Park, W.H.; Ihm, D.; Hudson, S.M. Effect of the degree of deacetylation on the thermal decomposition of chitin and chitosan nanofibers. *Carbohydr. Polym.* **2010**, *80*, 291–295, https://doi.org/10.1016/j.carbpol.2009.11.030.
49. Moussout, H.; Ahlafi, H.; Aazza, M.; Bourakhouadar, M. Kinetics and mechanism of the thermal degradation of biopolymers chitin and chitosan using thermogravimetric analysis. *Polym. Degrad. Stab.* **2016**, *130*, 1–9, https://doi.org/10.1016/j.polymdegradstab.2016.05.016.
50. Jang, M.K.; Kong, B.G.; Jeong, Y. Il; Lee, C.H.; Nah, J.W. Physicochemical characterization of α-chitin, β-chitin, and γ-chitin separated from natural resources. *J. Polym. Sci. Part A Polym. Chem.* **2004**, *42*, 3423–3432, https://doi.org/10.1002/pola.20176.
51. Kaya, M.; Mujtaba, M.; Ehrlich, H.; Salaberria, A.M.; Baran, T.; Amemiya, C.T.; Galli, R.; Akyuz, L.; Sargin, I.; Labidi, J. On chemistry of γ-chitin. *Carbohydr. Polym.* **2017**, *176*, 177–186,

https://doi.org/10.1016/j.carbpol.2017.08.076.
52. Ehrlich, H. Chitin and collagen as universal and alternative templates in biomineralization. *Int. Geol. Rev.* **2010**, *52*, 661–699, https://doi.org/10.1080/00206811003679521.
53. Kertmen, A.; Petrenko, I.; Schimpf, C.; Rafaja, D.; Petrova, O.; Sivkov, V.; Nekipelov, S.; Fursov, A.; Stelling, A.L.; Heimler, K. Calcite nanotuned chitinous skeletons of giant *ianthella basta* marine demosponge. *Int. J. Mol. Sci.* **2021**, *22*, https://doi.org/10.3390/ijms222212588.
54. Brunner, E.; Richthammer, P.; Ehrlich, H.; Paasch, S.; Simon, P.; Ueberlein, S.; Van Pée, K.H. Chitin-based organic networks: An integral part of cell wall biosilica in the diatom *thalassiosira pseudonana*. *Angew. Chemie - Int. Ed.* **2009**, *48*, 9724–9727, https://doi.org/10.1002/anie.200905028.
55. Bo, M.; Bavestrello, G.; Kurek, D.; Paasch, S.; Brunner, E.; Born, R.; Galli, R.; Stelling, A.L.; Sivkov, V.N.; Petrova, O. V. Isolation and identification of chitin in the black coral *Parantipathes larix* (*Anthozoa: Cnidaria*). *Int. J. Biol. Macromol.* **2012**, *51*, 129–137, https://doi.org/10.1016/j.ijbiomac.2012.04.016.
56. Nowacki, K.; Stępniak, I.; Langer, E.; Tsurkan, M.; Wysokowski, M.; Petrenko, I.; Khrunyk, Y.; Fursov, A.; Bo, M.; Bavestrello, G. Electrochemical approach for isolation of chitin from the skeleton of the black coral *cirrhipathes sp.* (*Antipatharia*). *Mar. Drugs* **2020**, *18*, https://doi.org/10.3390/md18060297.
57. Ehrlich, H.; Shaala, L.A.; Youssef, D.T.A.; Żółtowska-Aksamitowska, S.; Tsurkan, M.; Galli, R.; Meissner, H.; Wysokowski, M.; Petrenko, I.; Tabachnick, K.R. Discovery of chitin in skeletons of non-verongiid Red Sea demosponges. *PLOS One* **2018**, *13*, 1–18, https://doi.org/10.1371/journal.pone.0195803.
58. Kovalchuk, V.; Voronkina, A.; Binnewerg, B.; Schubert, M.; Muzychka, L.; Wysokowski, M.; Tsurkan, M. V.; Bechmann, N.; Petrenko, I.; Fursov, A. Naturally drug-loaded chitin: Isolation and applications. *Mar. Drugs* **2019**, *17*, 1–17, https://doi.org/10.3390/md17100574.
59. Schubert, M.; Binnewerg, B.; Voronkina, A.; Muzychka, L.; Wysokowski, M.; Petrenko, I.; Kovalchuk, V.; Tsurkan, M.; Martinovic, R.; Bechmann, N. Naturally prefabricated marine biomaterials: Isolation and applications of flat chitinous 3D scaffolds from *Ianthella labyrinthus* (*demospongiae: Verongiida*). *Int. J. Mol. Sci.* **2019**, *20*, https://doi.org/10.3390/ijms20205105.
60. Nowacki, K.; Stępniak, I.; Machałowski, T.; Wysokowski, M.; Petrenko, I.; Schimpf, C.; Rafaja, D.; Langer, E.; Richter, A.; Ziętek, J. Electrochemical method for isolation of chitinous 3D scaffolds from cultivated *Aplysina aerophoba* marine demosponge and its biomimetic application. *Appl. Phys. A Mater. Sci. Process.* **2020**, *126*, https://doi.org/10.1007/s00339-020-03533-2.
61. Talevski, T.; Talevska Leshoska, A.; Pejoski, E.; Pejin, B.; Machałowski, T.; Wysokowski, M.; Tsurkan, M. V.; Petrova, O.; Sivkov, V.; Martinovic, R. Identification and first insights into the structure of chitin from the endemic freshwater demosponge *Ochridaspongia rotunda* (Arndt, 1937). *Int. J. Biol. Macromol.* **2020**, *162*, 1187–1194, https://doi.org/10.1016/j.ijbiomac.2020.06.247.
62. Machałowski, T.; Wysokowski, M.; Żółtowska-Aksamitowska, S.; Bechmann, N.; Binnewerg, B.; Schubert, M.; Guan, K.; Bornstein, S.R.; Czaczyk, K.; Pokrovsky, O. Spider Chitin. The biomimetic potential and applications of *Caribena versicolor* tubular chitin. *Carbohydr. Polym.* **2019**, *226*, https://doi.org/10.1016/j.carbpol.2019.115301.
63. Machałowski, T.; Wysokowski, M.; Tsurkan, M. V; Galli, R.; Petrenko, I.; Czaczyk, K.; Kraft, M. Spider Chitin : An Ultrafast Microwave-Assisted. *Molecules* **2019**, *325*, https://doi.org/10.3390/molecules24203736.
64. Abdou, E.S.; Nagy, K.S.A.; Elsabee, M.Z. Extraction and characterization of chitin and chitosan from local sources. *Bioresour. Technol.* **2008**, *99*, 1359–1367, https://doi.org/10.1016/j.biortech.2007.01.051.
65. Kim, S.S.; Kim, S.J.; Moon, Y.D.; Lee, Y.M. Thermal characteristics of chitin and hydroxypropyl chitin. *Polymer (Guildf).* **1994**, *35*, 3212–3216, https://doi.org/10.1016/0032-3861(94)90124-4.
66. Kertmen, A.; Ehrlich, H. Patentology of chitinous biomaterials. Part I: Chitin. *Carbohydr. Polym.* **2022**, *282*, https://doi.org/10.1016/j.carbpol.2022.119102.
67. Tian, Z.; Wang, S.; Hu, X.; Zhang, Z.; Liang, L. Crystalline reduction, surface area enlargement and pore generation of chitin by instant catapult steam explosion. *Carbohydr. Polym.* **2018**, *200*, 255–261, https://doi.org/10.1016/j.carbpol.2018.07.075.
68. Kou, S.G.; Peters, L.M.; Mucalo, M.R. Chitosan: A review of sources and preparation methods. *Int. J. Biol. Macromol.* **2021**, *169*, 85–94, https://doi.org/10.1016/j.ijbiomac.2020.12.005.
69. Pereira, F.S.; Da Silva Agostini, D.L.; Job, A.E.; González, E.R.P. Thermal studies of chitin-chitosan derivatives. *J. Therm. Anal. Calorim.* **2013**, *114*, 321–327, https://doi.org/10.1007/s10973-012-2835-z.
70. Köll, P.; Borchers, G.; Metzger, J.O. Thermal degradation of chitin and cellulose. *J. Anal. Appl. Pyrolysis* **1991**, *19*, 119–129, https://doi.org/10.1016/0165-2370(91)80038-A.

71. Georgieva, V.; Zvezdova, D.;Vlaev, V. Non - isothermal kinetics of thermal degradation of chitin. *J. Therm. Anal. Calorim.* **2012**, https://doi.org/10.1007/s10973-012-2359-6.
72. Moreno-Tovar, R.; Bucio, L.; Thions, C.; Tehuacanero-Cuapa, S. Thermal degradation and lifetime of β-chitin from *Dosidicus gigas* squid pen: Effect of impact at 9.7 GPa and a comparative study with α-chitin. *Carb. Pol.* **2021**, https://doi.org/10.1016/j.carbpol.2020.116987.
73. Deguchi, S.; Tsujii, K.; Horikoshi, K. In situ microscopic observation of chitin and fungal cells with chitinous cell walls in hydrothermal conditions. *Nature*, **2015**, https://doi.org/10.1038/srep11907.
74. Ehrlich, H.; Rigby, J.K.; Botting, J.P.; Tsurkan, M. V.; Werner, C.; Schwille, P.; Petrášek, Z.; Pisera, A.; Simon, P.; Sivkov, V.N. Discovery of 505-million-year old chitin in the basal demosponge *Vauxia gracilenta*. *Sci. Rep.* **2013**, *3*, 17–20, https://doi.org/10.1038/srep03497.
75. Wysokowski, M.; Petrenko, I.; Stelling, A.L.; Stawski, D.; Jesionowski, T.; Ehrlich, H. Poriferan chitin as a versatile template for extreme biomimetics. *Polymers (Basel)* **2015**, *7*, 235–265, https://doi.org/10.3390/polym7020235.
76. Ehrlich, H.; Simon, P.; Motylenko, M.; Wysokowski, M.; Bazhenov, V. V.; Galli, R.; Stelling, A.L.; Stawski, D.; Ilan, M.; Stöcker, H. Extreme Biomimetics: Formation of zirconium dioxide nanophase using chitinous scaffolds under hydrothermal conditions. *J. Mater. Chem. B* **2013**, *1*, 5092–5099, https://doi.org/10.1039/c3tb20676a.
77. Wysokowski, M.; Motylenko, M.; Bazhenov, V.V.; Stawski, D.; Petrenko, I.; Ehrlich, A.; Behm, T.; Kljajic, Z.; Stelling, A.L.; Jesionowski, T. Poriferan chitin as a template for hydrothermal zirconia deposition. *Front. Mater. Sci.* **2013**, *7*, 248–260, https://doi.org/10.1007/s11706-013-0212-x.
78. Wysokowski, M.; Motylenko, M.; Stöcker, H.; Bazhenov, V.V.; Langer, E.; Dobrowolska, A.; Czaczyk, K.; Galli, R.; Stelling, A.L.; Behm, T. An extreme biomimetic approach: Hydrothermal synthesis of β-chitin/ZnO nanostructured composites. *J. Mater. Chem. B* **2013**, *1*, 6469–6476, https://doi.org/10.1039/c3tb21186j.
79. Wysokowski, M.; Behm, T.; Born, R.; Bazhenov, V.V.; Meißner, H.; Richter, G.; Szwarc-Rzepka, K.; Makarova, A.; Vyalikh, D.; Schupp, P. Preparation of chitin-silica composites by in vitro silicification of two-dimensional *Ianthella basta* demosponge chitinous scaffolds under modified Stöber conditions. *Mater. Sci. Eng. C* **2013**, *33*, 3935–3941, https://doi.org/10.1016/j.msec.2013.05.030.
80. Tsurkan, D.; Wysokowski, M.; Petrenko, I.; Voronkina, A.; Khrunyk, Y.; Fursov, A.; Ehrlich, H. Modern scaffolding strategies based on naturally pre-fabricated 3D biomaterials of poriferan origin. *Appl. Phys. A* **2020**, *126*, 382, https://doi.org/10.1007/s00339-020-03564-9.
81. Wysokowski, M.; Motylenko, M.; Walter, J.; Lota, G.; Wojciechowski, J.; Stöcker, H.; Galli, R.; Stelling, A.L.; Himcinschi, C.; Niederschlag, E. Synthesis of nanostructured chitin-hematite composites under extreme biomimetic conditions. *RSC Adv.* **2014**, *4*, 61743–61752, https://doi.org/10.1039/c4ra10017d.
82. Wysokowski, M.; Motylenko, M.; Beyer, J.; Makarova, A.; Stöcker, H.; Walter, J.; Galli, R.; Kaiser, S.; Vyalikh, D.; Bazhenov, V.V. Extreme biomimetic approach for developing novel chitin-GeO_2 nanocomposites with photoluminescent properties. *Nano Res.* **2015**, *8*, 2288–2301, https://doi.org/10.1007/s12274-015-0739-5.
83. Wysokowski, M.; Szalaty, T.J.; Jesionowski, T.; Motylenko, M.; Rafaja, D.; Koltsov, I.; Stöcker, H.; Bazhenov, V. V.; Ehrlich, H.; Stelling, A.L. Extreme biomimetic approach for synthesis of nanocrystalline chitin-(Ti/Zr)O_2 multiphase composites. *Mater. Chem. Phys.* **2017**, *188*, https://doi.org/10.1016/j.matchemphys.2016.12.038.
84. Wysokowski, M.; Machałowski, T.; Petrenko, I.; Schimpf, C.; Rafaja, D.; Galli, R.; Ziętek, J.; Pantović, S.; Voronkina, A.; Kovalchuk, V. 3D chitin scaffolds of marine demosponge origin for biomimetic mollusk hemolymph-associated biomineralization *ex-vivo*. *Mar. Drugs* **2020**, *18*, https://doi.org/10.3390/md18020123.
85. Petrenko, I.; Bazhenov, V.V.; Galli, R.; Wysokowski, M.; Fromont, J.; Schupp, P.J.; Stelling, A.L.; Niederschlag, E.; Stöker, H.; Kutsova, V.Z.; et al. Chitin of poriferan origin and the bioelectrometallurgy of copper/copper oxide. *Int. J. Biol. Macromol.* **2017**, *104*, 1626–1632, https://doi.org/10.1016/j.ijbiomac.2017.01.084.
86. Muzychka, L.; Voronkina, A.; Kovalchuk, V.; Smolii, O.B.; Wysokowski, M.; Petrenko, I.; Youssef, D.T.A.; Ehrlich, I.; Ehrlich, H. Marine biomimetics: bromotyrosines loaded chitinous skeleton as source of antibacterial agents. *Appl. Phys. A Mater. Sci. Process.* **2021**, *127*, 1–11, https://doi.org/10.1007/s00339-020-04167-0.
87. Klinger, C.; Żółtowska-Aksamitowska, S.Z.; Wysokowski, M.; Tsurkan, M. V.; Galli, R.; Petrenko, I.;

Machałowski, T.; Ereskovsky, A.; Martinović, R.; Muzychka, L. Express method for isolation of ready-to-use 3D chitin scaffolds from *aplysina archeri* (*aplysineidae: verongiida*) demosponge. *Mar. Drugs* **2019**, *17*, https://doi.org/10.3390/md17020131.

88. Santos, V.P.; Marques, N.S.S.; Maia, P.C.S.V.; de Lima, M.A.B.; Franco, L. de O.; de Campos-Takaki, G.M. Seafood waste as attractive source of chitin and chitosan production and their applications. *Int. J. Mol. Sci.* **2020**, *21*, 1–17, https://doi.org/10.3390/ijms21124290.
89. Aranaz, I.; Alcántara, A.R.; Civera, M.C.; Arias, C.; Elorza, B.; Caballero, A.H.; Acosta, N. Chitosan: An overview of its properties and applications. *Polymers (Basel)* **2021**, *13*, https://doi.org/10.3390/polym13193256.
90. Zawadzki, J.; Kaczmarek, H. Thermal treatment of chitosan in various conditions. *Carbohydr. Polym.* **2010**, *80*, 394–400, https://doi.org/10.1016/j.carbpol.2009.11.037.
91. Peniche-Covas, C.; Argüelles-Monal, W.; San Román, J. A kinetic study of the thermal degradation of chitosan and a mercaptan derivative of chitosan. *Polym. Degrad. Stab.* **1993**, *39*, 21–28, https://doi.org/10.1016/0141-3910(93)90120-8.
92. Muraleedharan, K.; Alikutty, P.; Abdul Mujeeb, V.M.; Sarada, K. Kinetic Studies on the Thermal Dehydration and Degradation of Chitosan and Citralidene Chitosan. *J. Polym. Environ.* **2015**, *23*, 1–10, https://doi.org/10.1007/s10924-014-0665-8.
93. López, F.A.; Mercê, A.L.R.; Alguacil, F.J.; López-Delgado, A. A kinetic study on the thermal behaviour of chitosan. *J. Therm. Anal. Calorim.* **2008**, *91*, 633–639, https://doi.org/10.1007/s10973-007-8321-3.
94. Gubanova, G.N.; Petrova, V.A.; Kononova, S.V.; Popova, E.N.; Smirnova, V.E.; Bugrov, A.N.; Klechkovskaya, V.V.; Skorik, Y.A. Thermal properties and structural features of multilayer films based on chitosan and anionic polysaccharides. *Biomolecules* **2021**, *11*, 1–15, https://doi.org/10.3390/biom11050762.
95. Corazzari, I.; Nisticò, R.; Turci, F.; Faga, M.G.; Franzoso, F.; Tabasso, S.; Magnacca, G. Advanced physico-chemical characterization of chitosan by means of TGA coupled on-line with FTIR and GCMS: Thermal degradation and water adsorption capacity. *Polym. Degrad. Stab.* **2015**, *112*, 1–9, https://doi.org/10.1016/j.polymdegradstab.2014.12.006.
96. Diab, M.A.; El-Sonbati, A.Z.; Bader, D.M.D.; Zoromba, M.S. Thermal Stability and Degradation of Chitosan Modified by Acetophenone. *J. Polym. Environ.* **2012**, *20*, 29–36, https://doi.org/10.1007/s10924-011-0330-4.
97. Szymańska, E.; Winnicka, K. Stability of chitosan - A challenge for pharmaceutical and biomedical applications. *Mar. Drugs* **2015**, *13*, 1819–1846, https://doi.org/10.3390/md13041819.
98. Grząbka-Zasadzińska, A.; Amietszajew, T.; Borysiak, S. Thermal and mechanical properties of chitosan nanocomposites with cellulose modified in ionic liquids. *J. Therm. Anal. Calorim.* **2017**, *130*, 143–154, https://doi.org10.1007/s10973-017-6295-3.
99. Zhang, Y.; Wu, Y.; Yang, M.; Zhang, G.; Ju, H. Thermal stability and dynamic mechanical properties of poly(ε-caprolactone)/chitosan composite membranes. *Materials (Basel)* **2021**, *14*, https://doi.org/10.3390/ma14195538.
100. Muley, A.B.; Chaudhari, S.A.; Mulchandani, K.H.; Singhal, R.S. Extraction and characterization of chitosan from prawn shell waste and its conjugation with cutinase for enhanced thermo-stability. *Int. J. Biol. Macromol.* **2018**, *111*, 1047–1058, https://doi.org/10.1016/j.ijbiomac.2018.01.115.
101. de Britto, D.; Campana-Filho, S.P. Kinetics of the thermal degradation of chitosan. *Thermochim. Acta* **2007**, *465*, 73–82, https://doi.org/10.1016/j.tca.2007.09.008.
102. Zeng, L.; Qin, C.; Wang, L.; Li, W. Volatile compounds formed from the pyrolysis of chitosan. *Carbohydr. Polym.* **2011**, *83*, 1553–1557, https://doi.org/10.1016/j.carbpol.2010.10.007.
103 Subramaniam, S.; Foo, K.Y.; Md Yusof, E.N.; Jawad, A.H.; Wilson, L.D.; Sabar, S. Hydrothermal synthesis of phosphorylated chitosan and its adsorption performance towards Acid Red 88 dye. *Int. J. Biol. Macromol.* **2021**, *193*, 1716–1726, https://doi.org/10.1016/j.ijbiomac.2021.11.009.
104. Sazali, M.S.; Yaakob, M.K.; Mohamed, Z.; Mamat, M.H.; Hassan, O.H.; Kaus, N.H.M.; Zu Azhan Yahya, M. Chitosan-assisted hydrothermal synthesis of multiferroic $BiFeO_3$: Effects on structural, magnetic and optical properties. *Results Phys.* **2019**, *15*, https://doi.org/10.1016/j.rinp.2019.102740.
105. Jia, S.; Pan, H.; Lin, Q.; Wang, X.; Li, C.; Wang, M.; Shi, Y. Study on the preparing and mechanism of chitosan-based nano-mesoporous carbons by hydrothermal method. *Nanotechnology* **2020**, https://doi.org/10.1088/1361-6528/ab9575.
106. Hileuskaya, K.S.; Mashkin, M.E.; Kraskouski, A.N.; Kabanava, V.S.; Stepanova, E.A.; Kuzminski, I.I.; Kulikouskaya, V.I.; Agabekov, V.E. Hydrothermal Synthesis and Properties of Chitosan–Silver

Nanocomposites. *Russ. J. Inorg. Chem.* **2021**, *66*, 1128–1134, https://doi.org/10.1134/S0036023621080064.
107. Jafari, H.; Mahdavinia, G.R.; Kazemi, B.; Ehrlich, H.; Joseph, Y.; Rahimi-Nasrabadi, M. Highly efficient sunitinib release from pH-responsive mHPMC@Chitosan core-shell nanoparticles. *Carbohydr. Polym.* **2021**, *258*, https://doi.org/10.1016/j.carbpol.2021.117719.
108. Badry, M.D.; Wahba, M.A.; Khaled, R.K.; Ali, M.M. Hydrothermally assisted synthesis of magnetic iron oxide-chitosan nanocomposites: Electrical and biological evaluation. *Biointerface Res. Appl. Chem.* **2022**, *12*, 2229–2241, https://doi.org/10.33263/BRIAC122.22292241.
109. Zhu, W.; Jiang, X.; Liu, F.; You, F.; Yao, C. Preparation of chitosan-graphene oxide composite aerogel by hydrothermal method and its adsorption property of methyl orange. *Polymers (Basel).* **2020**, *12*, https://doi.org/10.3390/POLYM12092169.
110. Akbari, M.; Jafari, H.; Rostami, M.; Mahdavinia, G.R.; Nasab, A.S.; Tsurkan, D.; Petrenko, I.; Ganjali, M.R.; Rahimi-Nasrabadi, M.; Ehrlich, H. Adsorption of cationic dyes on a magnetic 3D spongin scaffold with nano-sized Fe_3O_4 cores. *Mar. Drugs* **2021**, *19*, 1–20, https://doi.org/10.3390/MD19090512.
111. Szatkowski, T.; Siwínska-Stefańska, K.; Wysokowski, M.; Stelling, A.L.; Joseph, Y.; Ehrlich, H.; Jesionowski, T. Immobilization of titanium (IV) oxide onto 3D spongin scaffolds of marine sponge origin according to extreme biomimetics principles for removal of C.I. basic blue 9. *Biomimetics* **2017**, *2*, https://doi.org/10.3390/biomimetics2020004.
112. Żółtowska, S.; Modelska, M.; Piasecki, A.; Jesionowski, T. Commercial sponges in heterogeneous catalysis: developing novel composites with cobalt and silver. *Physicochem. Probl. Miner. Process.* **2020**, *56*, 89–100, https://doi.org/10.37190/ppmp/126866.
113. Khrunyk, Y.; Lach, S.; Petrenko, I.; Ehrlich, H. Progress in Modern Marine Biomaterials Research. *Mar. Drugs* **2020**, *18*, 1–46, https://doi.org/10.3390/md18120589.
114. Ehrlich, H.; Wysokowski, M.; Zółtowska-Aksamitowska, S.; Petrenko, I.; Jesionowski, T. Collagens of poriferan origin. *Mar. Drugs* **2018**, *16*, 1–21, https://doi.org/10.3390/md16030079.
115. Jesionowski, T.; Norman, M.; Zółtowska-Aksamitowska, S.; Petrenko, I.; Joseph, Y.; Ehrlich, H. Marine spongin: Naturally prefabricated 3D scaffold-based biomaterial. *Mar. Drugs* **2018**, *16*, 1–23, https://doi.org/10.3390/md16030088.
116. Norman, M.; Bartczak, P.; Zdarta, J.; Tomala, W.; Żurańska, B.; Dobrowolska, A.; Piasecki, A.; Czaczyk, K.; Ehrlich, H.; Jesionowski, T. Sodium copper chlorophyllin immobilization onto *Hippospongia communis* marine demosponge skeleton and its antibacterial activity. *Int. J. Mol. Sci.* **2016**, *17*, https://doi.org/10.3390/ijms17101564.
117. Norman, M.; Bartczak, P.; Zdarta, J.; Tylus, W.; Szatkowski, T.; Stelling, A.L.; Ehrlich, H.; Jesionowski, T. Adsorption of C.I. Natural Red 4 onto spongin skeleton of marine demosponge. *Materials (Basel).* **2015**, *8*, 96–116, https://doi.org/10.3390/ma8010096.
118. Żółtowska-Aksamitowska, S.; Koltsov, I.; Alejski, K.; Ehrlich, H.; Ciałkowski, M.; Jesionowski, T. Thermal decomposition behaviour and numerical fitting for the pyrolysis kinetics of 3D spongin-based scaffolds. The classic approach. *Polym. Test.* **2021**, *97*, https://doi.org/10.1016/j.polymertesting.2021.107148.
119. Antecka, K.; Zdarta, J.; Zgoła-Grześkowiak, A.; Ehrlich, H.; Jesionowski, T. Degradation of bisphenols using immobilized laccase supported onto biopolymer marine sponge scaffolds: Effect of operational parameters on removal efficiency. *N. Biotechnol.* **2018**, *44*, https://doi.org/10.1016/j.nbt.2018.05.1180.
120. Zdarta, J.; Antecka, K.; Frankowski, R.; Zgoła-Grześkowiak, A.; Ehrlich, H.; Jesionowski, T. The effect of operational parameters on the biodegradation of bisphenols by Trametes versicolor laccase immobilized on *Hippospongia communis* spongin scaffolds. *Sci. Total Environ.* **2018**, *615*, 784–795, https://doi.org/10.1016/j.scitotenv.2017.09.213.
121. Norman, M.; Bartczak, P.; Zdarta, J.; Ehrlich, H.; Jesionowski, T. Anthocyanin dye conjugated with *Hippospongia communis* marine demosponge skeleton and its antiradical activity. *Dye. Pigment.* **2016**, *134*, 541–552, https://doi.org/10.1016/j.dyepig.2016.08.019.
122. Szatkowski, T.; Kopczyński, K.; Motylenko, M.; Borrmann, H.; Mania, B.; Graś, M.; Lota, G.; Bazhenov, V.V.; Rafaja, D.; Roth, F. Extreme biomimetics: A carbonized 3D spongin scaffold as a novel support for nanostructured manganese (IV) oxide and its electrochemical applications. *Nano Res.* **2018**, *11*, 4199–4214, https://doi.org/10.1007/s12274-018-2008-x.
123. Zdarta, J.; Norman, M.; Smułek, W.; Moszyński, D.; Kaczorek, E.; Stelling, A.L.; Ehrlich, H.; Jesionowski, T. Spongin-based scaffolds from *Hippospongia communis* demosponge as an effective support for lipase immobilization. *Catalysts* **2017**, *7*, 1–20, https://doi.org/10.3390/catal7050147.
124. Szatkowski, T.; Wysokowski, M.; Lota, G.; Pęziak, D.; Bazhenov, V. V.; Nowaczyk, G.; Walter, J.;

Molodtsov, S.L.; Stöcker, H.; Himcinschi, C. Novel nanostructured hematite-spongin composite developed using an extreme biomimetic approach. *RSC Adv.* **2015**, *5*, 79031–79040, https://doi.org/10.1039/c5ra09379a.

125. Pozzolini, M.; Tassara, E.; Dodero, A.; Castellano, M.; Vicini, S.; Ferrando, S.; Aicardi, S.; Cavallo, D.; Bertolino, M.; Petrenko, I. Potential biomedical applications of collagen filaments derived from the marine demosponges *ircinia oros* (Schmidt, 1864) and *sarcotragus foetidus* (Schmidt, 1862). *Mar. Drugs* **2021**, *19*, https://doi.org/10.3390/md19100563.
126. Domingues, E.M.; Gonçalves, G.; Henriques, B.; Pereira, E.; Marques, P.A.A.P. High affinity of 3D spongin scaffold towards Hg (II) in real waters. *J. Hazard. Mater.* **2021**, *407*, https://doi.org/10.1016/j.jhazmat.2020.124807.
127. Tegza, M.; Andreyeva, O.; Maistrenko, L. Thermal analysis of collagen preparations. *Chem. Technol.* **2012**, *59*, 40–45, https://doi.org/10.5755/j01.ct.59.1.1528.
128. Notbohm, H.; Mosler, S.; Bodo, M.; Yang, C.; Lehmann, H.; Bätge, B.; Müller, P.K. Comparative study on the thermostability of collagen I of skin and bone: Influence of posttranslational hydroxylation of prolyl and lysyl residues. *J. Protein Chem.* **1992**, *11*, 635–643, https://doi.org/10.1007/BF01024964.
129. Wysokowski, M.; Petrenko, I.; Galli, R.; Schimpf, C.; Rafaja, D.; Hubalkova, J.; Aneziris, C.G.; Dyshlovoy, S.; von Amsberg, G.; Meissner, H. Extreme biomineralization: the case of the hypermineralized ear bone of gray whale (*Eschrichtius robustus*). *Appl. Phys. A Mater. Sci. Process.* **2020**, *126*, https://doi.org/10.1007/s00339-020-03913-8.
130. Wysokowski, M.; Zaslansky, P.; Ehrlich, H. Macrobiomineralogy: Insights and Enigmas in Giant Whale Bones and Perspectives for Bioinspired Materials Science. *ACS Biomater. Sci. Eng.* **2020**, *6*, 5357–5367, https://doi.org/10.1021/acsbiomaterials.0c00364.
131. Ehrlich, H.; Deutzmann, R.; Brunner, E.; Cappellini, E.; Koon, H.; Solazzo, C.; Yang, Y.; Ashford, D.; Thomas-Oates, J.; Lubeck, M. Mineralization of the metre-long biosilica structures of glass sponges is templated on hydroxylated collagen. *Nat. Chem.* **2010**, *2*, 1084–1088, https://doi.org/10.1038/nchem.899.
132. Wysokowski, M.; Jesionowski, T.; Ehrlich, H. Biosilica as a source for inspiration in biological materials science. *Am. Mineral.* **2018**, *103*, 665–691, https://doi.org/10.2138/am-2018-6429.
133. Du, C.; Wang, M.; Liu, J.; Pan, M.; Cai, Y.; Yao, J. Improvement of thermostability of recombinant collagen-like protein by incorporating a foldon sequence. *Appl. Microbiol. Biotechnol.* **2008**, *79*, 195–202, https://doi.org/10.1007/s00253-008-1427-0.
134. Dong, C.; Lv, Y. Application of collagen scaffold in tissue engineering: Recent advances and new perspectives. *Polymers (Basel).* **2016**, *8*, 1–20, https://doi.org/10.3390/polym8020042.
135. Chan, B.P.; So, K.F. Photochemical crosslinking improves the physicochemical properties of collagen scaffolds. *J. Biomed. Mater. Res. - Part A* **2005**, *75*, 689–701, https://doi.org/10.1002/jbm.a.30469.
136. Friess, W.; Lee, G. Basic thermoanalytical studies of insoluble collagen matrices. *Biomaterials* **1996**, *17*, 2289–2294, https://doi.org/10.1016/0142-9612(96)00047-6.
137. Pati, F.; Adhikari, B.; Dhara, S. Isolation and characterization of fish scale collagen of higher thermal stability. *Bioresour. Technol.* **2010**, *101*, 3737–3742, https://doi.org/10.1016/j.biortech.2009.12.133.
138. Wu, X.; Liu, Y.; Liu, A.; Wang, W. Improved thermal-stability and mechanical properties of type I collagen by crosslinking with casein, keratin and soy protein isolate using transglutaminase. *Int. J. Biol. Macromol.* **2017**, *98*, 292–301, https://doi.org/10.1016/j.ijbiomac.2017.01.127.
139. Leikina, E.; Mertts, M.V.; Kuznetsova, N.; Leikin, S. Type I collagen is thermally unstable at body temperature. *Proc. Natl. Acad. Sci. U. S. A.* **2002**, *99*, 1314–1318, https://doi.org/10.1073/pnas.032307099.
140. Trębacz, H.; Szczęsna, A.; Arczewska, M. Thermal stability of collagen in naturally ageing and *in vitro* glycated rabbit tissues. *J. Therm. Anal. Calorim.* **2018**, *134*, 1903–1911, https://doi.org/10.1007/s10973-018-7375-8.
141. Yang, J.; Ding, C.; Tang, L.; Deng, F.; Yang, Q.; Wu, H.; Chen, L.; Ni, Y.; Huang, L.; Zhang, M. Novel Modification of Collagen: Realizing Desired Water Solubility and Thermostability in a Conflict-Free Way. *ACS Omega* **2020**, *5*, 5772–5780, https://doi.org/10.1021/acsomega.9b03846.
142. Sankar, S.; Sekar, S.; Mohan, R.; Rani, S.; Sundaraseelan, J.; Sastry, T.P. Preparation and partial characterization of collagen sheet from fish (*Lates calcarifer*) scales. *Int. J. Biol. Macromol.* **2008**, *42*, 6–9, https://doi.org/10.1016/j.ijbiomac.2007.08.003.
143. Lim, J.J.; Shamos, M.H. Evaluation of kinetic parameters of thermal decomposition of native collagen by thermogravimetric analysis. *Biopolymers* **1974**, *13*, 1791–1807, https://doi.org/10.1002/bip.1974.360130912.
144. Patankar, K.C.; Maiti, S.; Singh, G.P.; Shahid, M.; More, S.; Adivarekar, R. V. Chemically modified wool

waste keratin for flame retardant cotton finishing. *Clean. Eng. Technol.* **2021**, *5*, https://doi.org/10.1016/j.clet.2021.100319.
145. Fudge, D.S.; Winegard, T.; Ewoldt, R.H.; Beriault, D.; Szewciw, L.; McKinley, G.H. From ultra-soft slime to hard α-keratins: The many lives of intermediate filaments. *Integr. Comp. Biol.* **2009**, *49*, 32–39, https://doi.org/10.1093/icb/icp007.
146. Alahyaribeik, S.; Ullah, A. Methods of keratin extraction from poultry feathers and their effects on antioxidant activity of extracted keratin. *Int. J. Biol. Macromol.* **2020**, *148*, 449–456, https://doi.org/10.1016/j.ijbiomac.2020.01.144.
147. Martínez-Hernández, A.L.; Velasco-Santos, C.; De Icaza, M.; Castaño, V.M. Microstructural characterisation of keratin fibres from chicken feathers. *Int. J. Environ. Pollut.* **2005**, *23*, 162–178, https://doi.org/10.1504/ijep.2005.006858.
148. Wrześniewska-Tosik, K.; Wesołowska, E.; Ryszkowska, J.; Montes, S.; Mik, T.; Kowalewski, T.; Kudra, M. Evaluation of the thermal stability of keratin fibres as a component of spun-bonded nonwovens for the manufacture of thermoset bio-based composites. *Fibres Text. East. Eur.* **2019**, *27*, 112–121, https://doi.org/10.5604/01.3001.0013.1827.
149. Brebu, M.; Spiridon, I. Thermal degradation of keratin waste. *J. Anal. Appl. Pyrolysis* **2011**, *91*, 288–295, https://doi.org/10.1016/j.jaap.2011.03.003.
150. Kakkar, P.; Madhan, B.; Shanmugam, G. Extraction and characterization of keratin from bovine hoof: A potential material for biomedical applications. *J. Korean Phys. Soc.* **2014**, *3*, 1–9, https://doi.org/10.1186/2193-1801-3-596.
151. Guo, Y.; Zhang, L.; Cao, F.; Leng, Y. Thermal treatment of hair for the synthesis of sustainable carbon quantum dots and the applications for sensing Hg^{2+}. *Sci. Rep.* **2016**, *6*, 1–7, https://doi.org/10.1038/srep35795.
152. Feroz, S.; Muhammad, N.; Ranayake, J.; Dias, G. Keratin - Based materials for biomedical applications. *Bioact. Mater.* **2020**, *5*, 496–509, https://doi.org/10.1016/j.bioactmat.2020.04.007.
153. Chilakamarry, C.R.; Mahmood, S.; Saffe, S.N.B.M.; Arifin, M.A. Bin; Gupta, A.; Sikkandar, M.Y.; Begum, S.S.; Narasaiah, B. Extraction and application of keratin from natural resources: a review. *3 Biotech* **2021**, *11*, 1–12, https://doi.org/10.1007/s13205-021-02734-7.
154. Sharma, S.; Gupta, A.; Kumar, A.; Kee, C.G.; Kamyab, H.; Saufi, S.M. An efficient conversion of waste feather keratin into ecofriendly bioplastic film. *Clean Technol. Environ. Policy* **2018**, *20*, 2157–2167, https://doi.org/10.1007/s10098-018-1498-2.
155. Valkov, A.; Zinigrad, M.; Sobolev, A.; Nisnevitch, M. Keratin biomembranes as a model for studying onychomycosis. *Int. J. Mol. Sci.* **2020**, *21*, https://doi.org/10.3390/ijms21103512.
156. Bechev, K.; Nikolov, G.; Kanchev, E. Thermal study of dyed chrome-treated keratin fibres. *J. Therm. Anal.* **1983**, *28*, 341–348, http://doi:10.1007/BF01983269.
157. Fortunati, E.; Aluigi, A.; Armentano, I.; Morena, F.; Emiliani, C.; Martino, S.; Santulli, C.; Torre, L.; Kenny, J.M.; Puglia, D. Keratins extracted from Merino wool and Brown Alpaca fibres: Thermal, mechanical and biological properties of PLLA based biocomposites. *Mater. Sci. Eng. C* **2015**, *47*, 394–406, https://doi.org/10.1016/j.msec.2014.11.007.
158. Zhang, J.; Li, Y.; Li, J.; Zhao, Z.; Liu, X.; Li, Z.; Han, Y.; Hu, J.; Chen, A. Isolation and characterization of biofunctional keratin particles extracted from wool wastes. *Powder Technol.* **2013**, *246*, 356–362, https://doi.org/10.1016/j.powtec.2013.05.037.
159. Senoz, E.; Wool, R.P.; McChalicher, C.W.J.; Hong, C.K. Physical and chemical changes in feather keratin during pyrolysis. *Polym. Degrad. Stab.* **2012**, *97*, 297–307, https://doi.org/10.1016/j.polymdegradstab.2011.12.018.
160. Kronenberger, K.; Dicko, C.; Vollrath, F. A novel marine silk. *Naturwissenschaften* **2012**, *99*, 3–10, https://doi.org/10.1007/s00114-011-0853-5.
161. Tokareva, O.; Jacobsen, M.; Buehler, M.; Wong, J.; Kaplan, D.L. Structure-function-property-design interplay in biopolymers: Spider silk. *Acta Biomater.* **2014**, *10*, 1612–1626, https://doi.org/10.1016/j.actbio.2013.08.020.
162. Hu, X.; Raja, W.K.; An, B.; Tokareva, O.; Cebe, P.; Kaplan, D.L. Stability of silk and collagen protein materials in space. *Sci. Rep.* **2013**, *3*, 1–3, https://doi.org/10.1038/srep03428.
163. Koh, L.D.; Cheng, Y.; Teng, C.P.; Khin, Y.W.; Loh, X.J.; Tee, S.Y.; Low, M.; Ye, E.; Yu, H.D.; Zhang, Y.W. Structures, mechanical properties and applications of silk fibroin materials. *Prog. Polym. Sci.* **2015**, *46*, 86–110, https://doi.org/10.1016/j.progpolymsci.2015.02.001.
164. Kiseleva, A.P.; Krivoshapkin, P. V.; Krivoshapkina, E.F. Recent Advances in Development of Functional

Spider Silk-Based Hybrid Materials. *Front. Chem.* **2020**, *8*, 1–20, https://doi.org/10.3389/fchem.2020.00554.
165. Strassburg, S.; Zainuddin, S.; Scheibel, T. The Power of Silk Technology for Energy Applications. *Adv. Energy Mater.* **2021**, *11*, https://doi.org/10.1002/aenm.202100519.
166. Katashima, T.; Malay, A.D.; Numata, K. Chemical modification and biosynthesis of silk-like polymers. *Curr. Opin. Chem. Eng.* **2019**, *24*, 61–68, https://doi.org/10.1016/j.coche.2019.01.005.
167. Blamires, S.J.; Spicer, P.T.; Flanagan, P.J. Spider Silk Biomimetics Programs to Inform the Development of New Wearable Technologies. *Front. Mater.* **2020**, *7*, 1–7, https://doi.org/10.3389/fmats.2020.00029.
168. Greco, G.; Francis, J.; Arndt, T.; Schmuck, B.; Bäcklund, F.G.; Barth, A.; Johansson, J.; Pugno, N.M.; Rising, A. Properties of biomimetic artificial spider silk fibers tuned by PostSpin bath incubation. *Molecules* **2020**, *25*, 1–11, https://doi.org/10.3390/molecules25143248.
169. Agnarsson, I.; Boutry, C.; Wong, S.C.; Baji, A.; Dhinojwala, A.; Sensenig, A.T.; Blackledge, T.A. Supercontraction forces in spider dragline silk depend on hydration rate. *Zoology* **2009**, *112*, 325–331, https://doi.org/10.1016/j.zool.2008.11.003.
170. Greco, G.; Mastellari, V.; Holland, C.; Pugno, N.M. Comparing modern and classical perspectives on spider silks and webs. *Perspect. Sci.* **2021**, *29*, 133–156, https://doi.org/10.1162/posc_a_00363.
171. Tsukada, M.; Arai, T.; Winkler, S.; Freddi, G.; Ishikawa, H. Physical properties of silk fibers grafted with vinyltrimethoxysilane. *J. Appl. Polym. Sci.* **2001**, *79*, 1764–1770, https://doi.org/10.1002/1097-4628(20010307)79:10<1764::AID-APP40>3.0.CO;2-E.
172. Gao, L.Z.; Bao, Y.; Cai, H.H.; Zhang, A.P.; Ma, Y.; Tong, X.L.; Li, Z.; Dai, F.Y. Multifunctional silk fabric via surface modification of nano-SiO_2. *Text. Res. J.* **2020**, *90*, 1616–1627, https://doi.org/10.1177/0040517519897112.
173. Hu, X.; Kaplan, D.; Cebe, P. Effect of water on the thermal properties of silk fibroin. *Thermochim. Acta* **2007**, *461*, 137–144, https://doi.org/10.1016/j.tca.2006.12.011.
174. Yazawa, K.; Ishida, K.; Masunaga, H.; Hikima, T.; Numata, K. Influence of Water Content on the β-sheet Formation, Thermal Stability, Water Removal, and Mechanical Properties of Silk Materials. *Biomacromolecules* **2016**, *17*, 1057–1066, https://doi.org/10.1021/acs.biomac.5b01685.
175. Prasong, S.; Yaowalak, S.; Wilaiwan, S. Characteristics of silk fiber with and without sericin component a comparision between Bombyx mori and Philosamia ricini Silks. *Pakistan J. Biol. Sci.* **2009**, *12*, 872–876, https://doi.org/10.3923/pjbs.2009.872.876.
176. Feng, X.X.; Zhang, L.L.; Chen, J.Y.; Guo, Y.H.; Zhang, H.P.; Jia, C.I. Preparation and characterization of novel nanocomposite films formed from silk fibroin and nano-TiO_2. *Int. J. Biol. Macromol.* **2007**, *40*, 105–111, https://doi.org/10.1016/j.ijbiomac.2006.06.011.
177. Wang, W.; Rather, L.J.; Gong, K.; Zhou, Q.; Zhang, T.; Li, Q. Effects of Ultrasonic Treatment on Hydrophilicity and Thermal Stability of Silk. *Macromol. Mater. Eng.* **2019**, *304*, 1–7, https://doi.org/10.1002/mame.201900364.
178. Bora, M.N.; Baruah, G.C.; Talukdar, C.L. Investigation on the thermodynamical properties of some natural silk fibres with various physical methods. *Thermochim. Acta* **1993**, *218*, 425–434, https://doi.org/10.1016/0040-6031(93)80441-C.
179. Jaramillo-Quiceno, N.; Álvarez-López, C.; Restrepo-Osorio, A. Structural and thermal properties of silk fibroin films obtained from cocoon and waste silk fibers as raw materials. *Procedia Eng.* **2017**, *200*, 384–388, https://doi.org/10.1016/j.proeng.2017.07.054.
180. Sacco, B.L.; Santana, H. Impact of temperature on the stability of silkworm cocoon fibers. *Artigo* **2019**, *XY*, 1–6, https://doi.org/10.21577/0100-4042.20170413.
181. Puerta, M.; Peresin, M.S.; Restrepo-Osorio, A. Effects of Chemical Post-treatments on Structural and Physicochemical Properties of Silk Fibroin Films Obtained From Silk Fibrous Waste. *Front. Bioeng. Biotechnol.* **2020**, *8*, 1–11, https://doi.org/10.3389/fbioe.2020.523949.
182. Benedict, C.V.; Waite, J.H. Composition and ultrastructure of the byssus of *Mytilus edulis*. *J. Morphol.* **1986**, *189*, 261–270, https://doi.org/10.1002/jmor.1051890305.
183. Tsukanda, M.; Gotoh, Y.; Yasuii, H.; Freddi, G.; Usuki, H. Comparison of chemical and physical properties of the byssus of *Mytilus edulis* with those of silk fibroin fibers. *J. Sericultural Sci. Japan* **1995**, *64*, 435–445, https://doi.org/10.11416/kontyushigen1930.64.435.
184. Torres, F.G.; Troncoso, O.P.; Ruiz, V. A thermomechanical study of elastomeric collagen-based fibers in the wet state. *Bioinspired, Biomim. Nanobiomaterials* **2013**, *2*, 93–97, https://doi.org/10.1680/bbn.13.00010.
185. Suhre, M.H.; Gertz, M.; Steegborn, C.; Scheibel, T. Structural and functional features of a collagen-binding matrix protein from the mussel byssus. *Nat. Commun.* **2014**, *5*, https://doi.org/10.1038/ncomms4392.

186. Harrington, M.J.; Jehle, F.; Priemel, T. Mussel Byssus Structure-Function and Fabrication as Inspiration for Biotechnological Production of Advanced Materials. *Biotechnol. J.* **2018**, *13*, 1–27, https://doi.org/10.1002/biot.201800133.
187. Torres, F.G.; Troncoso, O.P.; Torres, C.E. Mussel byssus fibres: A tough biopolymer. *RSC Green Chem.* **2012**, *1*, 305–329, https://doi.org/10.1039/9781849735193-00305.
188. Liu, W.; Yu, Z.; Huang, X.; Shi, Y.; Lin, J.; Zhang, H.; Yi, X.; He, M. Effect of ocean acidification on growth, calcification, and gene expression in the pearl oyster. *Pinctada fucata*. *Mar. Environ. Res.* **2017**, *130*, 174–180, https://doi.org/10.1016/j.marenvres.2017.07.013.
189. Nicklisch, S.C.T.; Waite, J.H. Mini-review: The role of redox in Dopa-mediated marine adhesion. *Biofouling* **2012**, *28*, 865–877, https://doi.org/10.1080/08927014.2012.719023.
190. Priemel, T.; Degtyar, E.; Dean, M.N.; Harrington, M.J. Rapid self-assembly of complex biomolecular architectures during mussel byssus biofabrication. *Nat. Commun.* **2017**, *8*, 1–12, https://doi.org/10.1038/ncomms14539.
191. Amstad, E.; Harrington, M.J. From vesicles to materials: Bioinspired strategies for fabricating hierarchically structured soft matter. *Philos. Trans. R. Soc. A Math. Phys. Eng. Sci.* **2021**, *379*, https://doi.org/10.1098/rsta.2020.0338.
192. Voss-Foucart, M.F.; Gregoire, Ch. On biochemical and structural alterations of the nacre conchiolin in the nautilus shell under conditions of protracted, moderate heating and pressure. *Arch. Physiol. Biochem.* **1975**, *83*, 43–52, https://doi.org/10.3109/13813457509069838.
193. Voss-Foucart, M.F.; Gregoire, Ch. Experimental alteration of the Nautilus shell by factors of diagenesis and metamorphism, Part II - Amino acid patterns in the conchiolin matrix of the pyrolysed modern mother-of-pearl. *Biologie* **1973**.
194. Gregoire, Ch. Experimental alteration of the Nautilus shell by factors involved in diagenesis and metamorphism, Part I - Thermal changes in conchiolin matrix of mother-of-pearl. *Biologie* **1968**.
195. Ehrlich, H.; Martinović, R.; Joksimović, D.; Petrenko, I.; Schiaparelli, S.; Wysokowski, M.; Tsurkan, D.; Stelling, A.L.; Springer, A.; Gelinsky, M. *Conchixes*: organic scaffolds which resemble the size and shapes of mollusks shells, their isolation and potential multifunctional applications. *Appl. Phys. A Mater. Sci. Process.* **2020**, *126*, 1–13, https://doi.org/10.1007/s00339-020-03728-7.
196. Eglinton, G.; Murphy, M.T.J. Organic Geochemistry, 1st ed.; Springer-Verlag, Berlin, Heidelberg **1969**, pp. 498-519, https://doi.org/10.1007/978-3-642-87734-6.
197. Gregoire, Ch. Thermal Changes in the Nautillus Shell. *Nature* **1964**, *204*, 868–869.